

General Disclaimer

One or more of the Following Statements may affect this Document

- This document has been reproduced from the best copy furnished by the organizational source. It is being released in the interest of making available as much information as possible.
- This document may contain data, which exceeds the sheet parameters. It was furnished in this condition by the organizational source and is the best copy available.
- This document may contain tone-on-tone or color graphs, charts and/or pictures, which have been reproduced in black and white.
- This document is paginated as submitted by the original source.
- Portions of this document are not fully legible due to the historical nature of some of the material. However, it is the best reproduction available from the original submission.

(NASA-TM-86104) TORTUOSITY OF LIGHTNING
RETURN STROKE CHANNELS (NASA) 67 p
HC A04/MF A01

N84-28295

CSCL 04A

Unclas

G3/47 19687



Technical Memorandum TM 86104

TORTUOSITY OF LIGHTNING RETURN STROKE CHANNELS

D. M. Le Vine and Bruce Gilson

MAY 1984

National Aeronautics and
Space Administration

Goddard Space Flight Center
Greenbelt, Maryland 20771



TORTUOSITY OF LIGHTNING RETURN STROKE CHANNELS

D. M. Le Vine
Environmental Sensors Branch
Goddard Laboratory for Atmospheric Sciences
Goddard Space Flight Center

Bruce Gilson
Computer Science Corporation
Silver Spring, MD

May 1984

GODDARD SPACE FLIGHT CENTER
Greenbelt, Maryland

ABSTRACT

Data obtained from photographs of lightning are presented on the tortuosity of return stroke channels. The data were obtained by making piecewise linear fits to the channels, and recording the cartesian coordinates of the ends of each linear segment. The mean change between ends of the segments was nearly zero in the horizontal direction and was about 8 meters in the vertical direction. Histograms of these changes are presented.

These data have been used to create model lightning channels and to predict the electric fields radiated during return strokes. This was done using a computer generated random walk in which linear segments are placed end-to-end to form a piecewise linear representation of the channel. The computer selects random numbers for the ends of the segments assuming a normal distribution with the measured statistics. Once the channels have been simulated, the electric fields radiated during a return stroke are predicted using a transmission line model on each segment. It is found that realistic channels are obtained with this procedure, but only if the model includes two scales of tortuosity: fine scale irregularities corresponding to the local channel tortuosity which are superimposed on large scale horizontal drifts. The two scales of tortuosity are also necessary to obtain agreement between the electric fields computed mathematically from the simulated channels and the electric fields radiated from real return strokes. Without large scale drifts the computed electric fields do not have the undulations characteristic of the data.

PRECEDING PAGE BLANK NOT FILMED

TORTUOSITY OF LIGHTNING RETURN STROKE CHANNELS

I. INTRODUCTION

Most of the recent attempts to model lightning return strokes have been based on what is called in the literature on lightning a "transmission line" model. This model was initially proposed by Dennis and Pierce (1964) to satisfy requirements for conservation of charge and was later extensively developed for application to return strokes by Uman and colleagues (Uman et al., 1973; Uman and McLain, 1969; McLain and Uman, 1971). The model represents the return stroke by a pulse of current propagating at constant velocity along a straight, usually vertical, path. However, it is clear, even to the casual observer, that the channels of lightning return strokes are highly irregular paths. It has been shown that including the channel geometry in models of the return stroke can noticeably affect predictions for the radiated electromagnetic fields. This was pointed out by R. D. Hill (1968, 1969) for VLF radiation and at higher frequencies by Le Vine and Meneghini (1978a, b). Recently, Le Vine and Gessel (1984) showed the importance of channel tortuosity on the output of AM radio receiver tuned to radio frequencies between 3 and 300 MHz. The effect of channel tortuosity is to add to the smooth electromagnetic field waveforms predicted by the transmission line model, the irregular variations characteristic of measurements (Le Vine and Meneghini, 1978a; Tiller et al., 1976; Weidman and Krider, 1978; Lin et al., 1979). Ribner and Roy (1981) also found that including channel tortuosity was important in properly predicting thunder from model channels.

The purpose of this paper is to present data on the tortuosity of return stroke channels, and then to show that this data can be used to simulate realistic lightning channels and that these channels lead to predictions for the electromagnetic fields radiated during return strokes which are consistent with observation. The data were obtained from photographs of lightning return strokes by fitting the channels with small linear segments (e.g. making a piecewise linear

fit) and recording the cartesian coordinates of the segment's end points. Histograms of the change in coordinates between end points will be presented in the section to follow. The histograms are suggestive of a normal distribution, and the data yield mean changes in the horizontal direction of close to zero meters and in the vertical direction of about 8 meters with a standard deviation of 5.6 and 6.1 meters, respectively. Following a procedure originally demonstrated by Le Vine and Meneghini (1978a) this data can be used to obtain computer simulations of the channels. In this procedure the computer creates a model channel by placing linear segments end-to-end in a random walk. The procedure is suggestive of the manner in which return stroke channels are created in real lightning by the stepped leader. It will be shown that using the data obtained from the photographs, leads to realistic lightning channels. However, it is concluded that a random walk with two probability distributions is required to obtain realistic looking channels. The two distributions give the channel large scale drifts upon which small scale fluctuations are superimposed. The piecewise linear simulation has also been used to calculate the electromagnetic fields radiated during a return stroke. To do so, each linear segment is treated as a small transmission line model (i.e. a current pulse is assumed to propagate along the segment at constant velocity); however, unlike conventional transmission line models, with the piecewise linear representation of the channel the parameters of the model can change from segment to segment. In the final section of this paper examples are presented of the electric fields predicted with the model channels. It is shown that the large scale fluctuations add undulations to the predicted electric fields which are characteristic of electric fields radiated from real return strokes.

II. DATA

The data base for this study is a collection of photographs of lightning return strokes copied from the archives at the University of New Mexico Institute of Mining and Technology in Socorro, New Mexico. About 25 photographs were selected from this collection, most of them streak camera photographs of return stroke channels. From this set 8 were selected for analysis. The selection was based on channel length and optical quality of the image. It was desired to obtain long channels with a minimum of exposure so that high spatial resolution could be obtained. The eight channels were isolated from the remainder of the photograph by removing branches or nearby subsequent return strokes. These channels, labelled A-H are shown in Figures 1-4. (The crosses are a grid superimposed on the photographs as a reference.) The original photographs from which these channels were selected are shown in Appendix A. Prior to analysis, each channel was enlarged so that it was 41" long. Then the enlargement was divided into 6 sections for convenience in the analysis. Figure 5 shows (on the right) the upper most section of the enlargement for channel C.

The analysis consisted of making a piecewise linear fit to the channel and recording the coordinates of the junctions where the segments met. This was done by hand by first placing a coordinate grid (e.g. the cartesian grid of graph paper) over the channel to establish a coordinate reference, and then following the channel with a straight edge until the straight line deviated from the channel by half the optical width of the channel. The X-coordinate (horizontal) and Z-coordinate (vertical) of this point were recorded. Then the straight edge was reoriented to again follow the channel. On the left in Figure 5 are shown the junction points and piecewise linear fit for the section of channel C shown on the right. The data obtained in this manner consisted of pairs of points (X,Z) identifying the junctions. However, only the changes between points are characteristic of the channel (the reference is arbitrary) and so the data were recorded as pairs (ΔX , ΔZ) of the change in coordinates in going from one junction point to the next. A complete listing of these data for the 8 channels is given in Appendix B.

To give an idea of the statistical nature of ΔX and ΔZ , histograms were prepared to show their relative frequency of occurrence. Histograms for the composite data set are given in Figures 6-7 and histograms for each individual channel are presented in Appendix C. In the histograms the units on the abscissa are arbitrary units chosen to equal the spacing between the lines on the grid used to measure the coordinates of the ends of the linear segments. (This grid was the same for all channels.) This distance can be converted to meters if the channel length, L , in meters and the number, N , of grid lines per inch is known. Thus, knowing that each photograph was 41 inches long, one obtains the scale factor: $L/41N = \text{distance in meters between grid lines}$. Although L is not known for these data, an estimate can be made by assuming that in each photograph the entire channel between cloud base and ground is shown. Assuming that the cloud base near Socorro, New Mexico to be about 1.5 km one obtains ($N = 20$ lines per inch) a value of about 2.0 meters for the width of the cells in the histogram. This is also the order of magnitude of the optical width of the channel in each photograph. Using this scale factor it is seen from Figure 7 that the greatest horizontal change for any segment was on the order of 20 meters and that the channel had a slight tendency to drift to left (negative). The mean change in horizontal position from segment to segment for the composite data set was about -0.26 meters. On the other hand, the vertical changes for this channel (Figure 6) were predominately positive and an average 8.46 meters long. The largest change was about 36 meters (positive = up) and there were a few cases where the channel appeared to reverse direction ($\Delta Z < 0$). Table I lists the mean and standard deviation of ΔX and ΔZ for each channel and also for the composite data set. The data is given in arbitrary units. For the composite data set $\langle \Delta Z \rangle = 4.23$ units, $\langle \Delta X \rangle = -0.13$ units and $\sigma_z = 3.04$ and $\sigma_x = 2.82$ units. Notice that the histograms for the horizontal displacement ΔX of each segment are suggestive of a normal distribution. A plot of the cumulative distribution on probability paper also supports this suggestion; consequently, some preliminary statistical tests for normal distributions were made. However the results were mixed and generally the hypothesis of a normal distribution is not accepted at high confidence levels. Several tests were also made for statistical independence of the ΔX and ΔZ . These indicated very strongly

that the horizontal variations ΔX and vertical variations ΔZ were uncorrelated. However, the autocorrelation of the horizontal and vertical variations themselves is not zero. Values of the correlation coefficient for the channels are given in Table I.

Table 1
Channel Statistics

Channel	$\langle \Delta Z \rangle$	σ_z	$\langle \Delta X \rangle$	σ_x	Autocorrelation		Number of Segments
					ΔX	ΔZ	
A	3.36	2.28	-0.10	2.26	—	—	204
B	4.33	2.93	-0.42	2.64	—	—	179
C	4.06	3.13	-0.70	2.95	.49	.13	244
D	4.65	2.87	1.05	2.70	.48	.17	215
E	3.99	3.57	-1.74	3.05	.36	.38	252
F	4.77	3.14	-1.39	2.76	.35	.13	209
G	4.84	3.12	1.19	3.08	.45	.22	206
H	3.87	3.11	1.09	3.03	.48	.18	259
Average	4.23	3.04	-0.13	2.82	.44	.20	221

III. CHANNEL MODELLING

As described by Le Vine and Meneghini (1978a, b), a computer generated representation for the channel can be obtained by placing linear segments end-to-end in a random walk. If, assuming that during a return stroke a current pulse propagates at constant velocity along each segment, this model is what is called in the literature on lightning a transmission line model; however, in this case with the flexibility to include channel geometry and changes in velocity of propagation or other parameters as the current advances from segment to segment along the channel.

In order to implement this model it is convenient to let the computer select the changes (ΔX , ΔY , ΔZ) of the cartesian coordinates that occur in going from one segment to the next. This is conveniently accomplished by having the computer select numbers at random from a collection with a prescribed probability distribution. The analysis described in the previous section suggests that as an initial hypothesis one assume that the ΔX , ΔY , ΔZ are normally distributed, independent, random variables. The normal distribution is a convenient distribution which is commonly encountered in nature in situations involving large numbers of independent trials, and so seems reasonable as a beginning assumption. The justification will be in the amount of agreement the model obtains with real lightning channels.

Figure 8 shows several channels generated using the piecewise linear model assuming normally distributed ΔX , ΔY , and ΔZ assuming $\langle \Delta X \rangle = \langle \Delta Y \rangle = 0$ and $\langle \Delta Z \rangle = 8\text{m}$ and letting $\sigma_z = 6\text{m}$ which are values obtained from the data for the eight channels (Table I). In Figure 8C the standard deviation of the horizontal coordinates ΔX and ΔY are also $\sigma_x = \sigma_y = 6\text{m}$ and in Figure 8D the standard deviation is somewhat lower $\sigma_x = \sigma_y = 4\text{m}$. Otherwise the two sets of channels in Figures 8C and 8D are generated from the same distribution and have the same mean horizontal displacement (ΔX and ΔY) and vertical displacement (ΔZ). In each case about 300 segments were used to generate the channel (220 was typical of the data). Notice that the channels with horizontal displacements with the larger standard deviation (Row C) show a greater degree of small scale wig-

gliness (tortuosity). However, if ΔZ were not the same for these two sets of channels, the tortuosity would not necessarily appear to be greater to the eye. This is true because the angle a segment makes with the vertical depends on both ΔZ and $\sqrt{\Delta X^2 + \Delta Y^2}$. In general it proved difficult to obtain a quantitative measure of tortuosity which agreed with the visual impression; however, the following parameter proved useful in the studies: $T = \sigma_x / \langle \Delta Z \rangle$. This parameter was adopted a priori, but it does have some justification. In particular, in one dimension σ_x is the mean-square length of the horizontal displacements (because $\langle \Delta X \rangle = 0$), and so T is the ratio of the mean horizontal length in one dimension to the mean vertical length of each segment. Consequently T is an indication of the angle that the segment makes with the vertical. It is dimensionless and therefore also is independent of the scale. As a result channels with long or short segments and the same T will appear to have roughly the same wiggleness. This parameter was about 0.44 for the real lightning channels. It is 0.50 for the channels in Figure 8D and is 0.75 for the channels in Figure 8C.

Five of the real lightning channels (D – F) are also displayed in Figure 8 (Row B). Notice that the real lightning channels not only have small scale tortuosity as in the simulated channels but also exhibit a drift to the right or left which changes direction as one moves up the channel. The real channels behave as if the horizontal displacement locally has a mean value which is different in different portions of the channel. The simulated channels, in contrast, are very nearly vertical with very little evidence of horizontal drifts, as indeed one would expect with the assumption $\langle \Delta X \rangle = \langle \Delta Z \rangle = 0$.

In a channel with a tendency for variations of a small scale to be superimposed on a structure of a larger scale, there will be a corresponding tendency for a number of consecutive changes (e.g. ΔX or ΔY) to be close in value. This will manifest itself as a high degree of correlation between the changes of adjacent segments. This correlation (i.e. the autocorrelation) was computed for both the simulated channels and the data obtained from the photographs of real lightning return strokes. Calculations were made of the autocorrelation coefficient of both ΔX and ΔZ . The values for the data are shown

in Table 1. For the simulated channels the autocorrelation was zero, as was to be expected since independent choices were made by the computer for the zero mean random numbers representing the ends of the linear segments. In the real channels the autocorrelation for the horizontal changes ΔX was on the order of 0.44 (Table 1). One way of obtaining simulated channels with correlated horizontal displacements is to assign non-zero values to the mean for ΔX and ΔY . Since the drifts in the real channels seem to be different for different parts of the channels, it was decided to allow the means to be themselves random variables. These new random variables were assumed to be zero mean and normally distributed with standard deviation σ_x and σ_y . The σ_x and σ_y were chosen by trial and error to achieve correlation coefficients of about .45 for the simulated channels. The simulation was modified so that it chose from a zero mean, normal distribution random numbers for the values of $\langle \Delta X \rangle$ and $\langle \Delta Y \rangle$ and independently from another normal distribution choose the points along the channel at which these means were to be changed. Figure 8A shows five channels generated in this manner. Notice the presence of drifts to the left and right in these simulated channels and the obviously improved agreement with the real lightning channels. The channels in Figure 8A have the same means, standard deviation and autocorrelation as the data as well as having the same tortuosity parameter $T = .44$.

IV. THE RADIATED ELECTRIC FIELD WAVEFORM

The large scale fluctuations not only improve the visual agreement between the model channels and photographs of lightning, they also improve the agreement between the radiated electric field waveforms predicted mathematically using the model channels and measurements of electric fields radiated from real return strokes. The measurements indicate that the electric fields radiated to a distant observer during a return stroke begin abruptly and then decay irregularly (Tiller et al., 1976, Weidman and Krider, 1978; Lin et al., 1978) in a process lasting about 100 μ s. Two examples are shown in Figure 10 which are representative of data collected by Le Vine in Florida in July, 1978, during the TRIP experiment (Pierce, 1976). The data were obtained using a field change system designed by Krider (e.g. Krider et al., 1977; Le Vine and Krider, 1977). Notice that although the decay of the electric field waveform is irregular, a pattern of peaks and valleys is clearly evident. This is a feature which is characteristic of the electric field waveforms radiated from first return strokes (Weidman and Krider, 1978). This feature is also present in the simulations obtained with model channels, but only when the large scale fluctuations are included in the model. Without the large scale fluctuations the decay consists of a rather smooth envelope upon which are superimposed small changes.

Techniques for calculating the electric fields radiated during return strokes using a piecewise linear model for the channel have been described by Le Vine and Meneghini (1978 a,b). These techniques assumes that during the return stroke current propagates along each linear segment of the model channel at constant speed. As described above, this amounts to a piecewise linear version of what is called a "transmission line" model in the literature on lightning. In the version of this model employed here, a solution is obtained for the radiation from each segment using a Fraunhofer approximation (e.g. Le Vine and Meneghini, 1978 a,b); then the computer obtains the total electric field at the observation point by using this solution to sum the contribution from each segment, keeping track of the location of the current pulse as it propagates along the channel.

Figures 10 and 11 show several examples obtained with this simulation. The channel is shown to the left and the electric field calculated for a point on the surface 100 km from the channel is shown to the right. It has been assumed that the ground plane is perfectly conducting ($\sigma = \infty$). Two examples are shown in each figure. On the top is the electric field computed from a channel which includes large scale fluctuations and on the bottom is shown the electric field computed from a channel which is identical (i.e. was obtained from the same statistical distribution using the same random seeds) except that the fluctuations in the mean of the horizontal segment length, used to obtain the large scale changes in the channel, have been omitted. The result is a distinctively straighter channel as was discussed in the preceding sections. The difference is also clearly reflected in the electric field waveforms shown to the right. The electric field predicted in either case rises abruptly at the beginning of the return stroke; however, in the absence of the large scale fluctuations, the decay has a monotonic envelope upon which are superimposed small irregular changes, whereas when the large scale fluctuations are included in the channel, the envelope of the electric field waveform exhibits large undulations as it decays. These undulations are easily correlated with changes in the large scale geometry of the channels. Their presence gives the radiated electric field waveform a shape more representative of the data than the waveforms obtained when the large scale changes are absent (bottom of each figure). The examples shown in Figures 10 and 11 are representative of calculations made on several different channels. The current waveform used in the calculations is the exponential model described in Le Vine and Meneghini (1978a).

V. CONCLUSIONS

A study has been made of the tortuosity of lightning return stroke channels using a piecewise linear fit to the channel. It was found that the mean vertical change in length was about 8 meters and that the mean in the horizontal direction was nearly zero. The standard deviation in both the vertical and horizontal directions were about 6 m. However, simulations of lightning channels using segments chosen at random from a normal distribution with these parameters are relatively straight and do not have the large scale bends found in real lightning channels. Large scale bends can be simulated by allowing the mean of the horizontal changes in segment position to vary at random. Doing so not only yields channels which appear to the eye to be more representative of real lightning but also yield channels whose correlation (between the changes in length from one segment to the next) is consistent with the data. In the simulations the means were chosen by selecting numbers at random from a zero mean, normal distribution with standard deviation $\sigma = 6.58$.

The large scale bends not only yield realistic looking channels, but also improve agreement between data from real lightning and the electric fields calculated from model return strokes. The large scale bends add to the calculated electric fields large undulations in the decaying portions of the waveform as is characteristic of the data. Large scale variations in the channel geometry were also found to be necessary by Ribner and Roy (1981) to achieve successful simulations of thunder from model channels.

REFERENCES

- Dennis, A. S., and E. T. Pierce, "The Return Stroke of the Lightning Flash to Earth as a Source of VLF Atmospherics," *Radio Science*, 68D (No. 7), pp. 777-794, 1964.
- Hill, R. D., "Electromagnetic Radiation from Erratic Paths of Lightning Strokes," *J. Geophys. Res.*, 74 (#8), pp. 1922-1929, 1969.
- Hill, R. D., "Analysis of Irregular Paths of Lightning Channels," *J. Geophys. Res.*, 73, pp. 1897-1906, 1968.
- Krider, E. P., C. D. Weidman, and R. C. Noggle, "The Electric Fields Produced by Lightning Stepped Leaders," *J. Geophys. Res.*, 82, 951-960, 1977.
- Le Vine, D. M. and L. Gessel, "The Influence of Ground Conductivity on the Structure of RF Radiation from Return Strokes," Presented at the VII International Conference on Atmospheric Electricity, Albany, NY, June, 1984 (Also NASA TM-86065).
- Le Vine, D. M. and E. P. Krider, "The Temporal Structure of HF and VHF Radiations During Florida Lightning Return Strokes," *Geophys. Res. Lett.*, 4, pp. 13-16, 1977.
- Le Vine, D. M. and R. Meneghini, "Simulations of Radiation from Lightning Return Strokes: The Effects of Tortuosity," *Radio Science*, 13, p. 801, 1978a.
- Le Vine, D. M. and R. Meneghini, "Electromagnetic Fields Radiated from a Lightning Return Stroke: Application of an Exact Solution to Maxwell's Equations," *J. Geophys. Res.*, 83, pp. 2377-2384, 1978b.

- Lin, Y. T., M. A. Uman, J. A. Tiller, R. D. Brantley, W. H. Beasley, E. P. Krider, and C. D. Weidman, "Characterization of Lightning Return Stroke Electric and Magnetic Fields from Simultaneous Two-Station Measurements," J. Geophys. Res., *84 (C10)*, pp. 6307-6314, 1979.
- McLain, D. K., and M. A. Uman, "Exact Expression and Moment Approximation for the Electric Field Intensity of the Lightning Return Stroke," J. Geophys. Res., *76 (No. 9)*, pp. 2101-2105, 1971.
- Pierce, E. T., "The Thunderstorm Research International Program (TRIP)—1976", Bull. Amer. Meteorol. Soc. *57*, pp. 1214-1216, 1976.
- Ribner, H. S., and D. Roy, "Thunder from Tortuous Lightning: A Computer Model Mode Audible," Proc. AIAA 7th Aeroacoustics Conference, Palo Alto, California, October 5-7, 1981.
- Tiller, J. A., M. A. Uman, Y. T. Lin, R. D. Brantley and E. P. Krider, "Electric Field Statistics for Close Lightning Return Strokes near Gainesville, Florida," J. Geophys. Res., *81*, pp. 4430-4434, 1976.
- Uman, M. A., D. K. McLain, R. J. Fisher and E. P. Krider, "Electric Field Intensity of the Lightning Return Stroke," J. Geophys. Res., *78 (No. 18)*, pp. 3523-3529, 1973.
- Uman, M. A. and D. K. McLain, "Magnetic Field of Lightning Return Stroke," J. Geophys. Res., *74 (No. 28)*, pp. 6899-6910, 1969.
- Weidman, C. D. and E. P. Krider, "The Fine Structure of Lightning Return Strokes Waveforms," J. Geophys. Res., *83*, pp. 6239-6247, 1978.

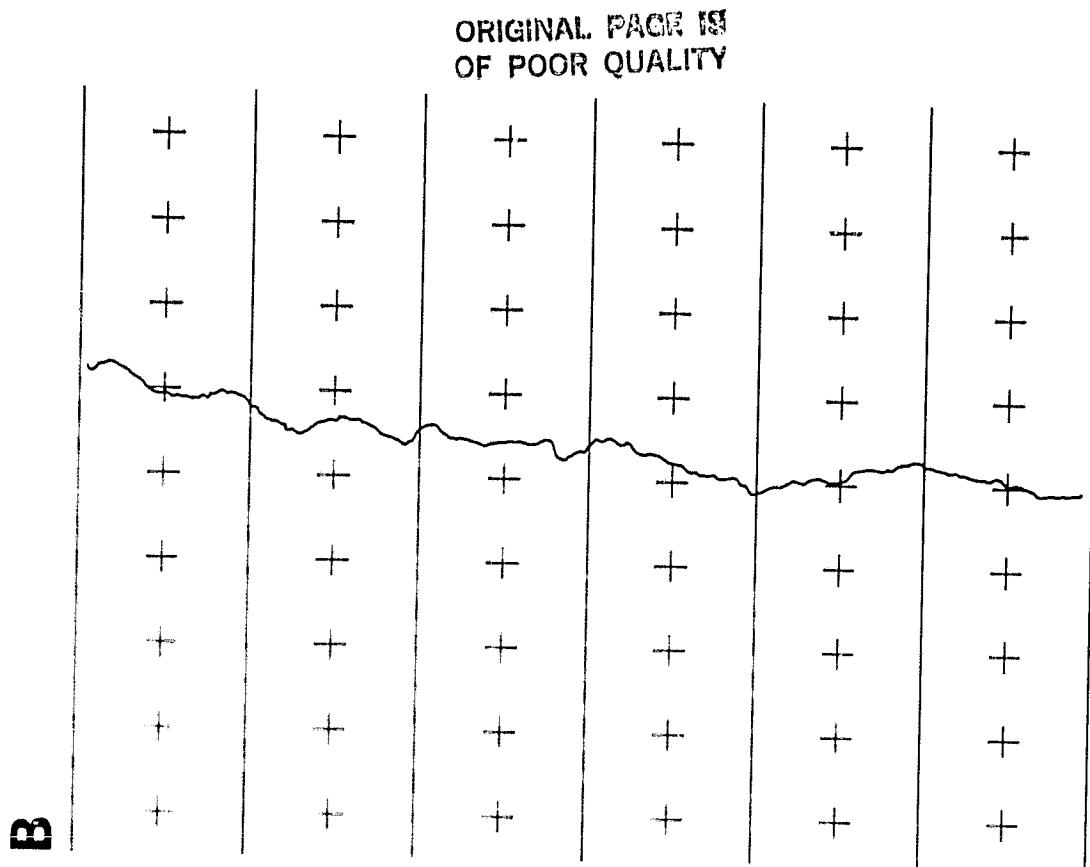
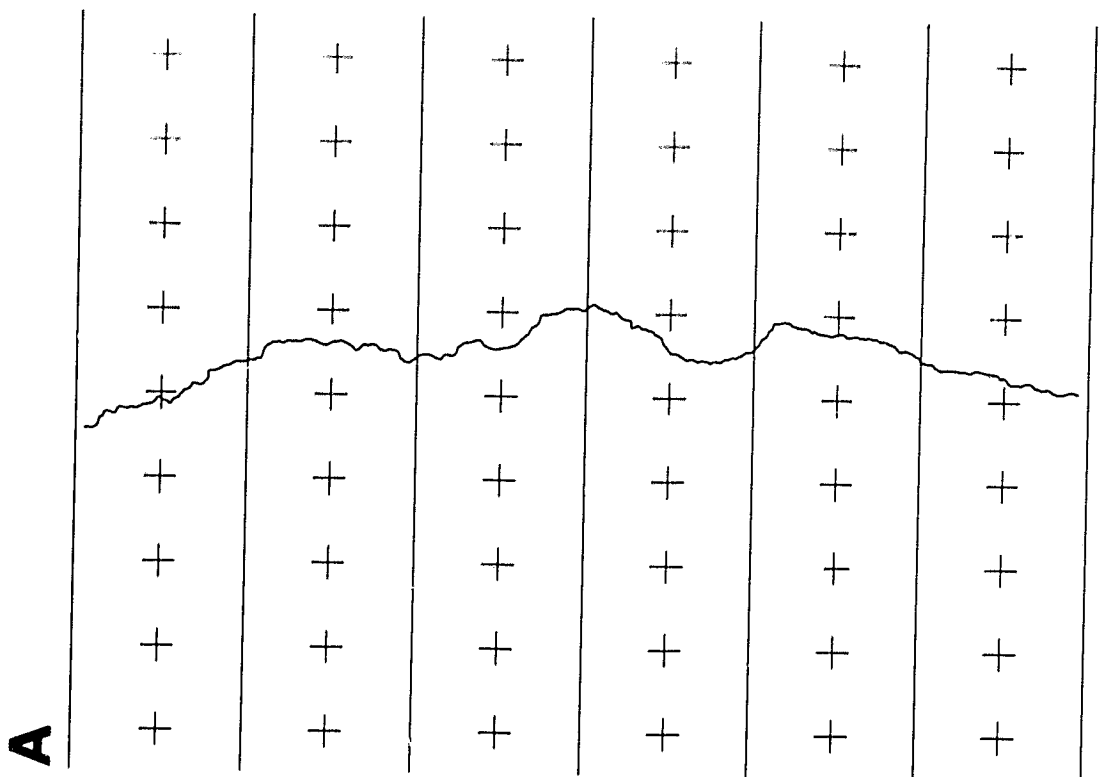


Figure 1. Channels A and B. The lines and crosses are a spatial reference used in analysis.

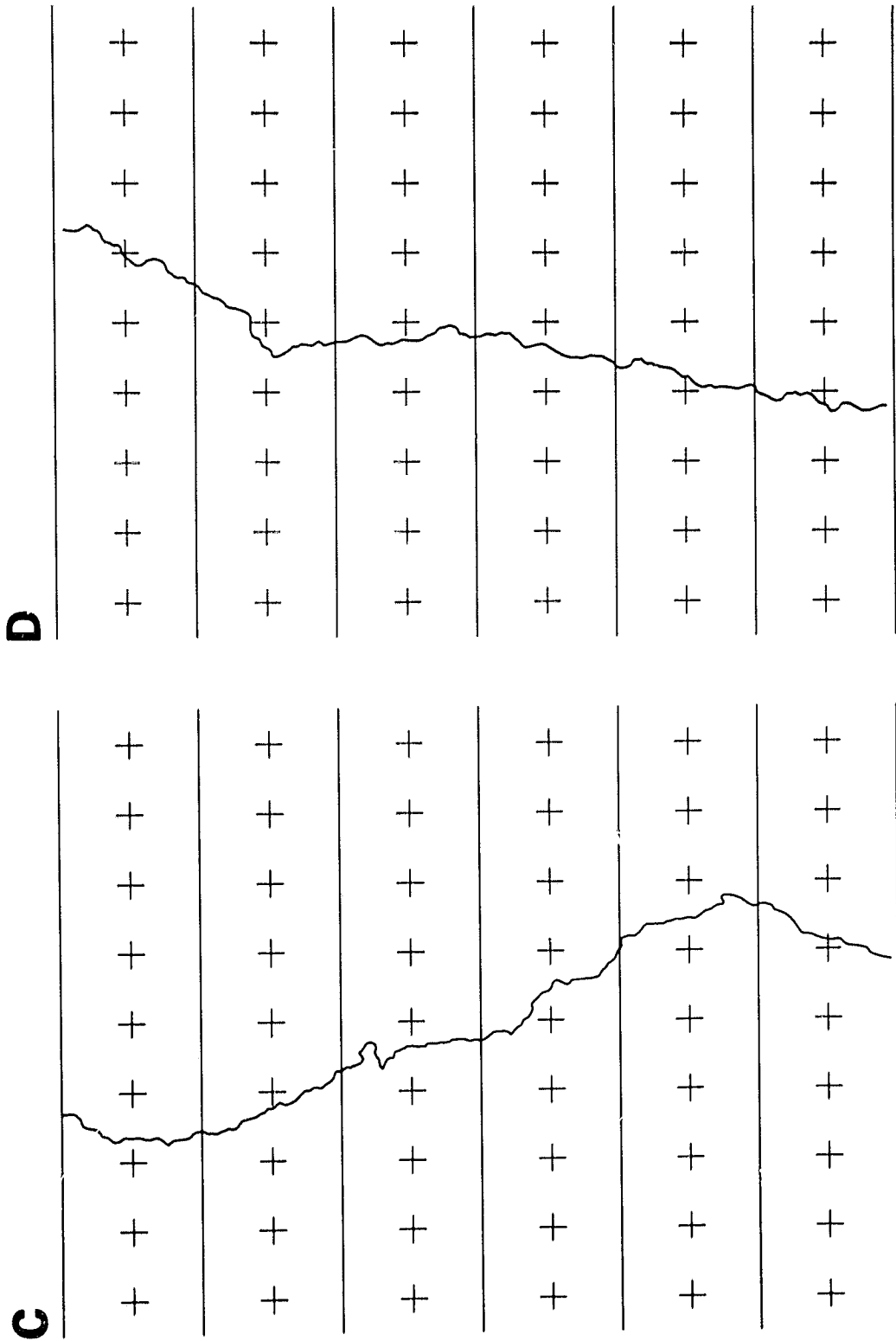


Figure 2. Channels C and D. The lines and crosses are a spatial reference for use in analysis.

ORIGINAL PAGE IS
OF POOR QUALITY

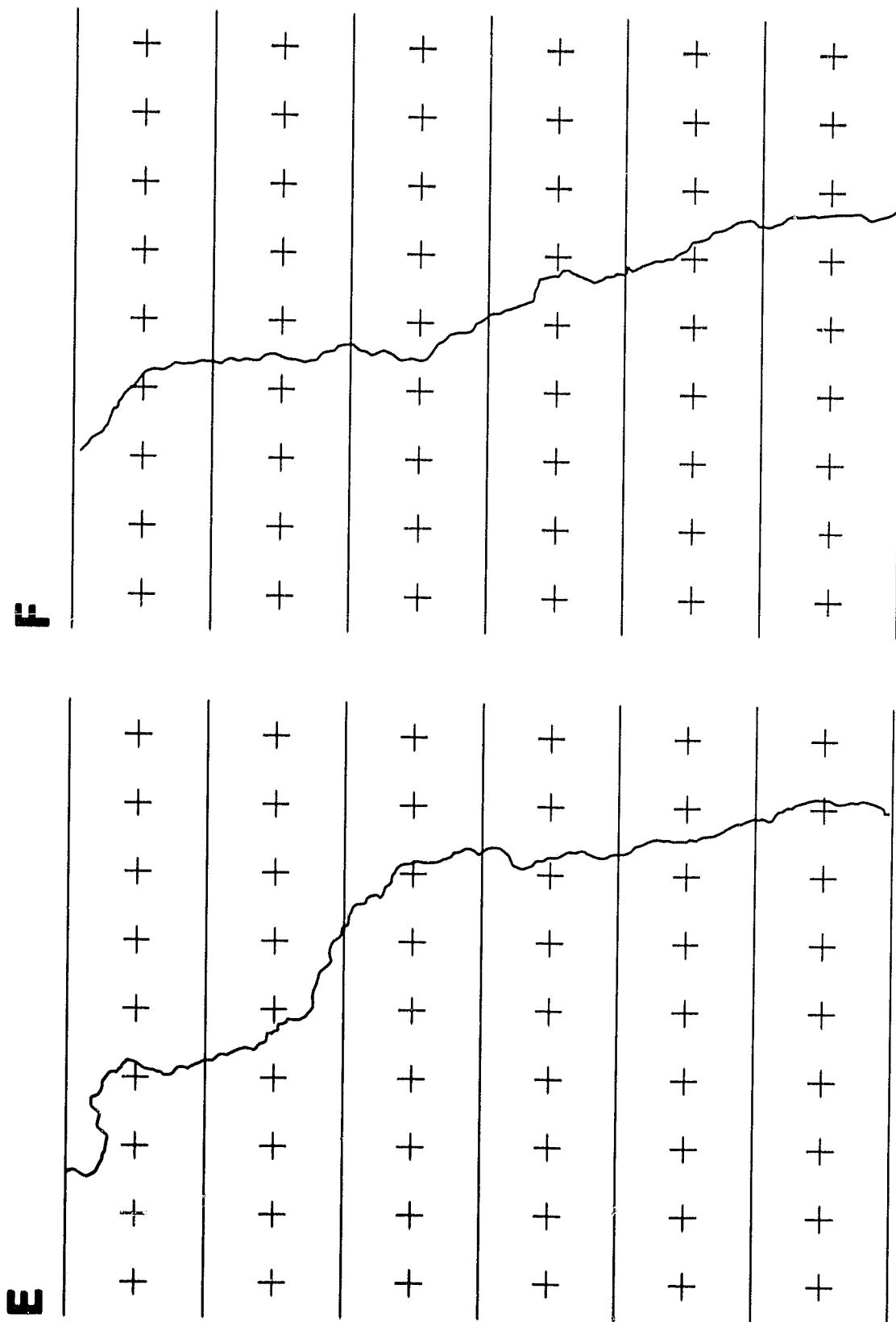


Figure 3. Channels E and F. The lines and crosses were added to provide a spatial reference for the analysis.

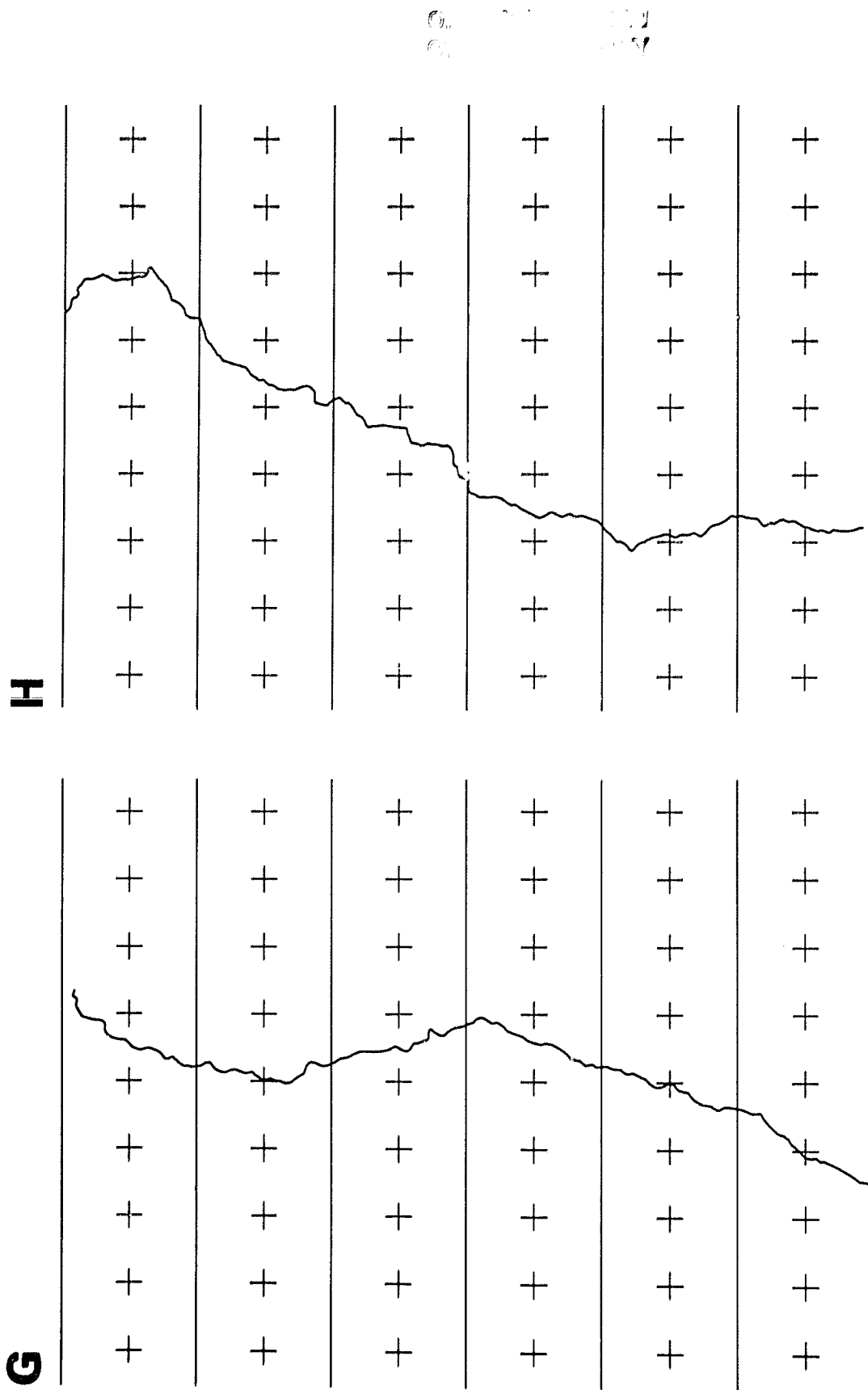
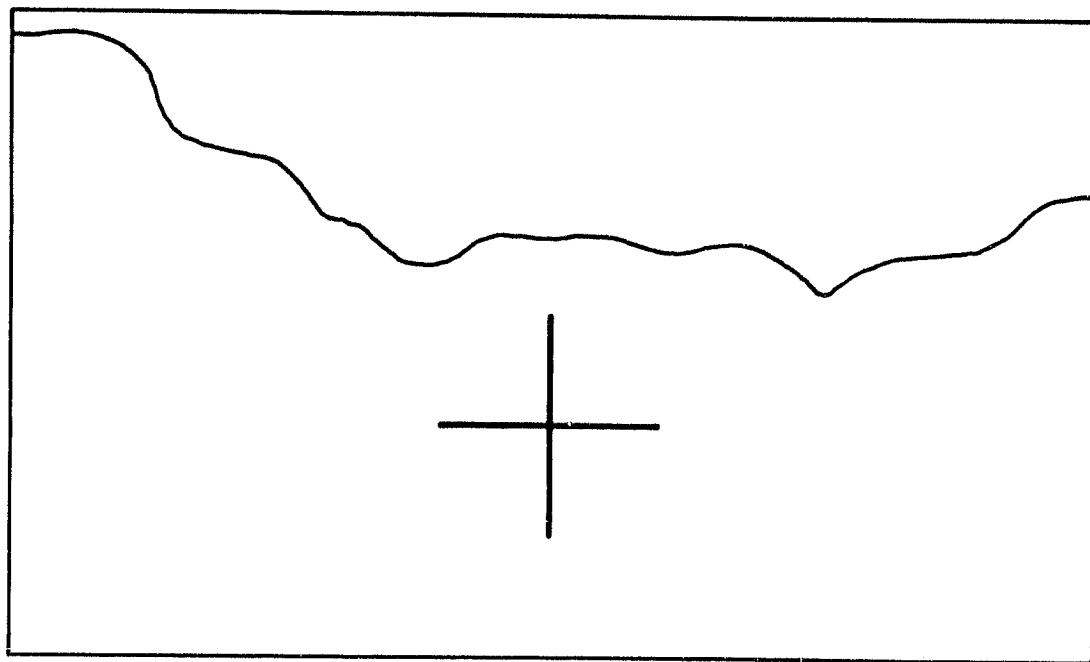


Figure 4. Channels G and H. The lines and crosses were added to provide a spatial reference for the analysis.

ORIGINAL PAGE IS
OF POOR QUALITY

CHANNEL



LINEAR PIECES

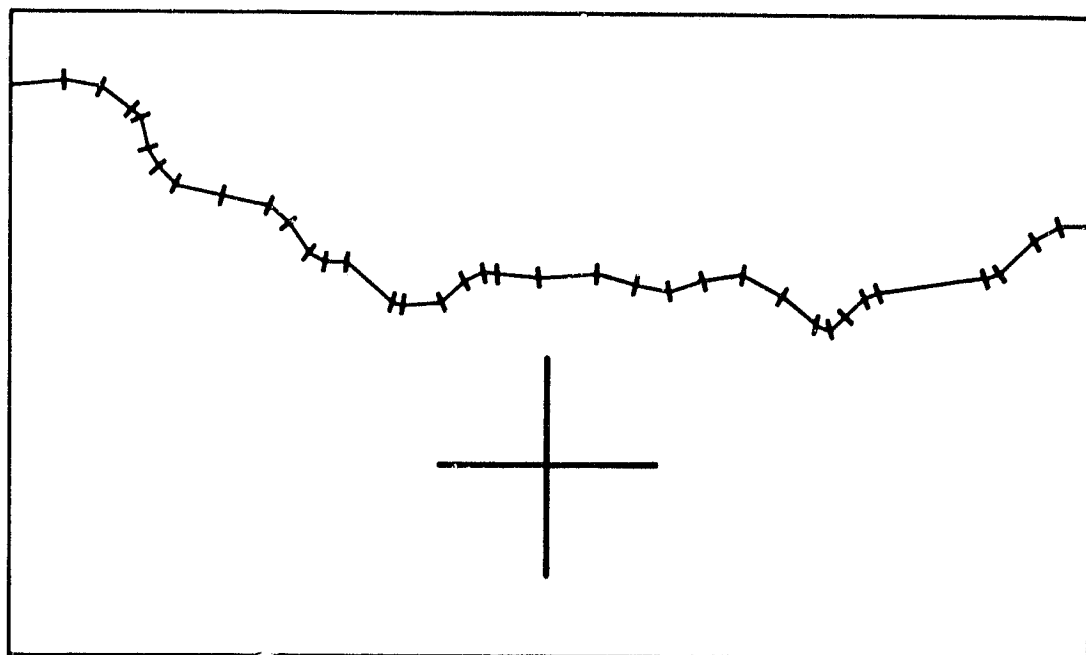


Figure 5. The upper most section (portion between horizontal lines) of channel C is shown on the right. On the left is the piecewise linear fit to this piece of channel.

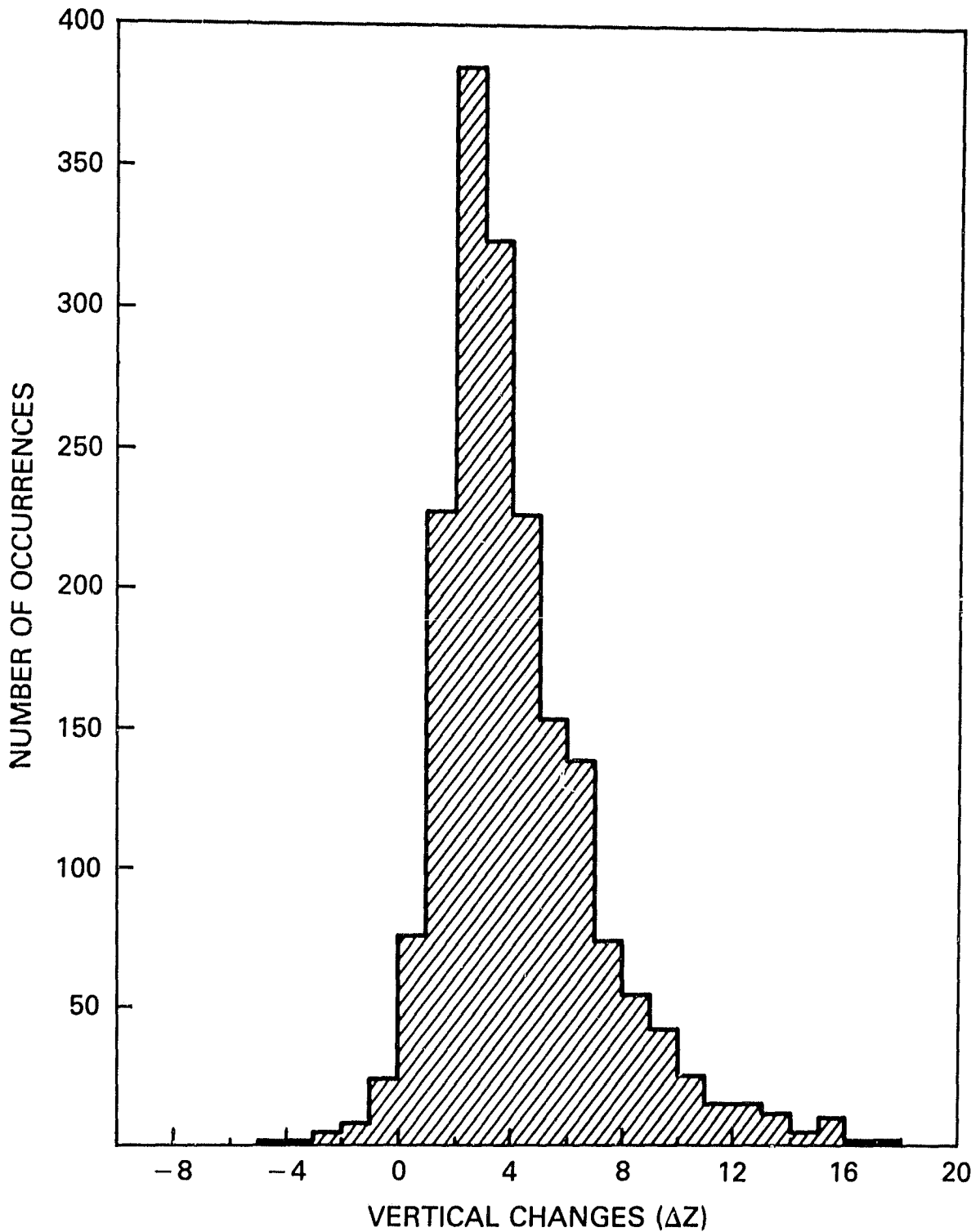


Figure 6. Composite histogram of the change in vertical coordinate (ΔZ) between ends of the segments in a piecewise linear fit to the channels. This histogram is for channels A-H.

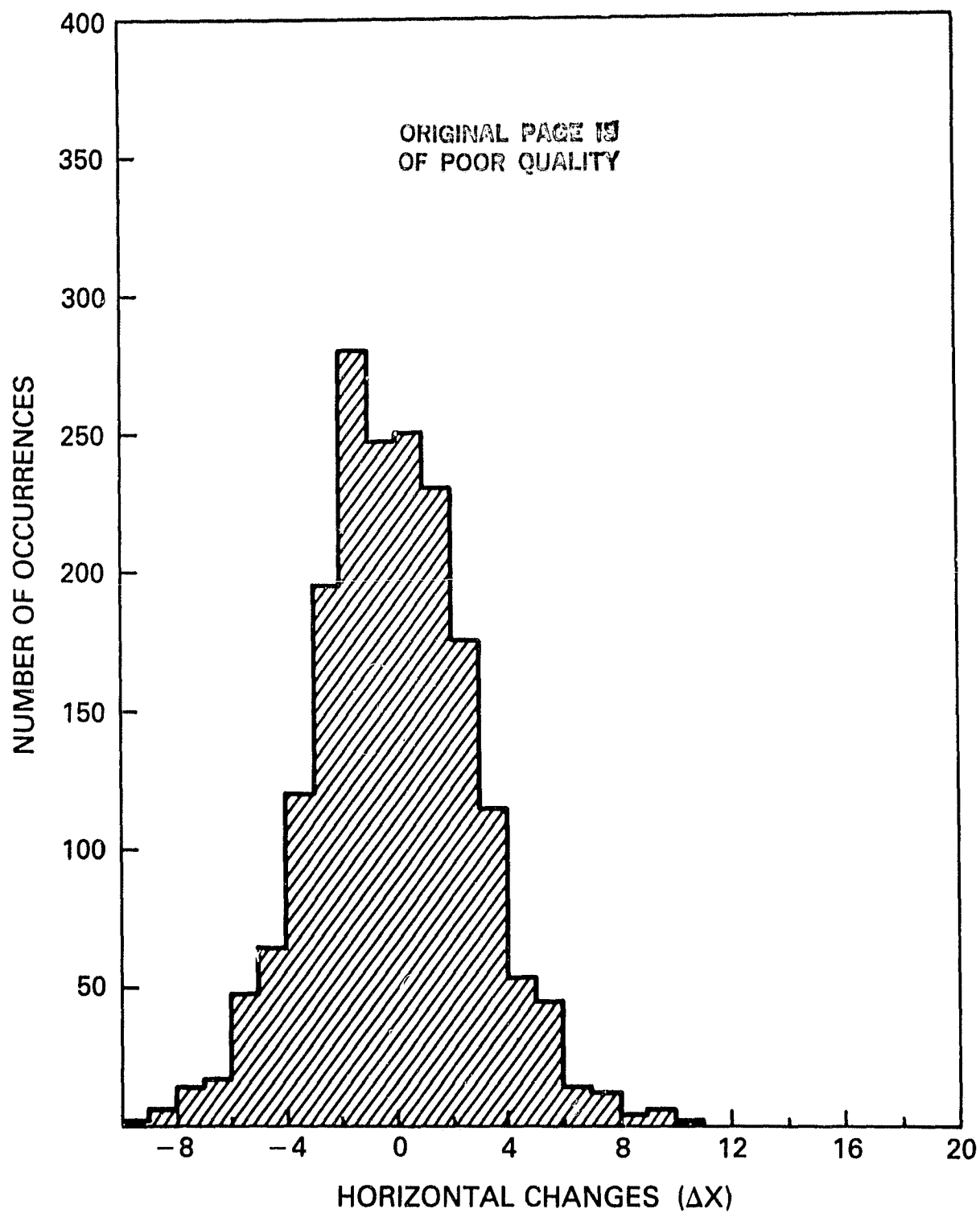


Figure 7. Composite histogram of the horizontal changes (ΔX) between ends of the segment in the piecewise linear fit to the channels. This histogram is for channels A-H.

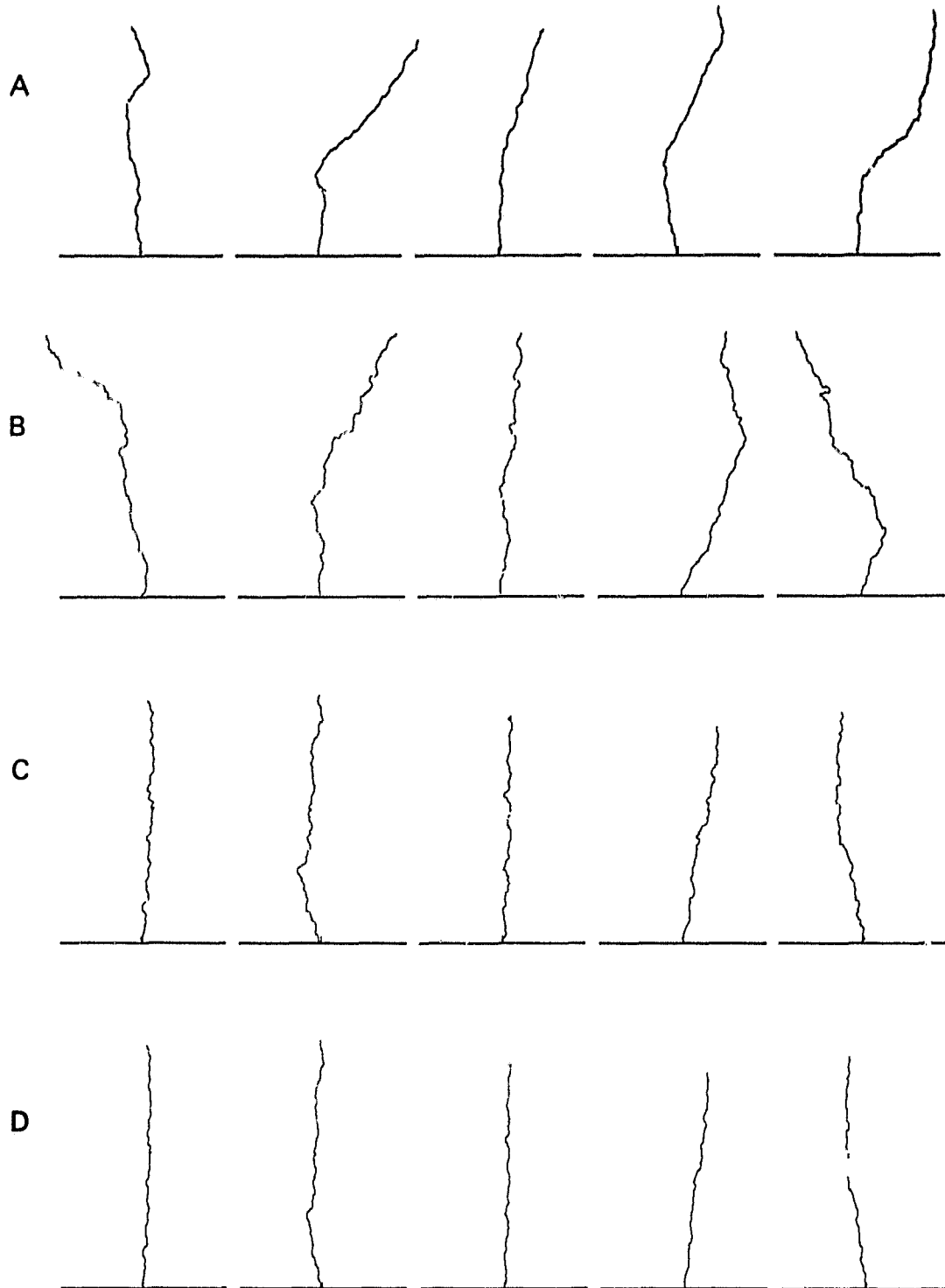


Figure 8. Examples of return stroke channels. Rows A, C and D are simulations. Row B are channels of real lightning return strokes. Each row of the simulations is generated from the same statistical distributions.

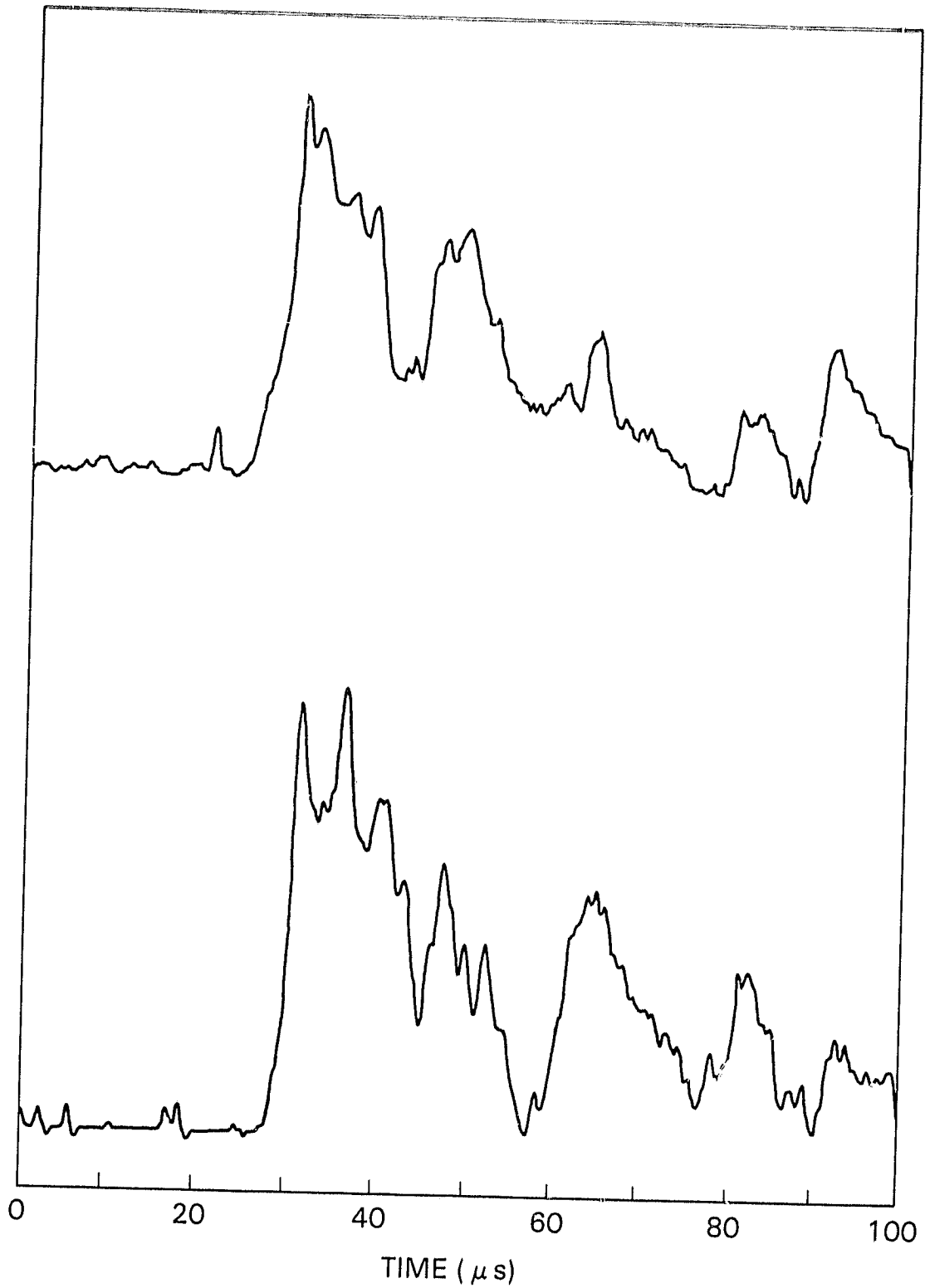


Figure 9. Electric field waveforms from first return strokes. These data were collected in Florida during TRIP-78 (July, 1978) at the Kennedy Space Center.

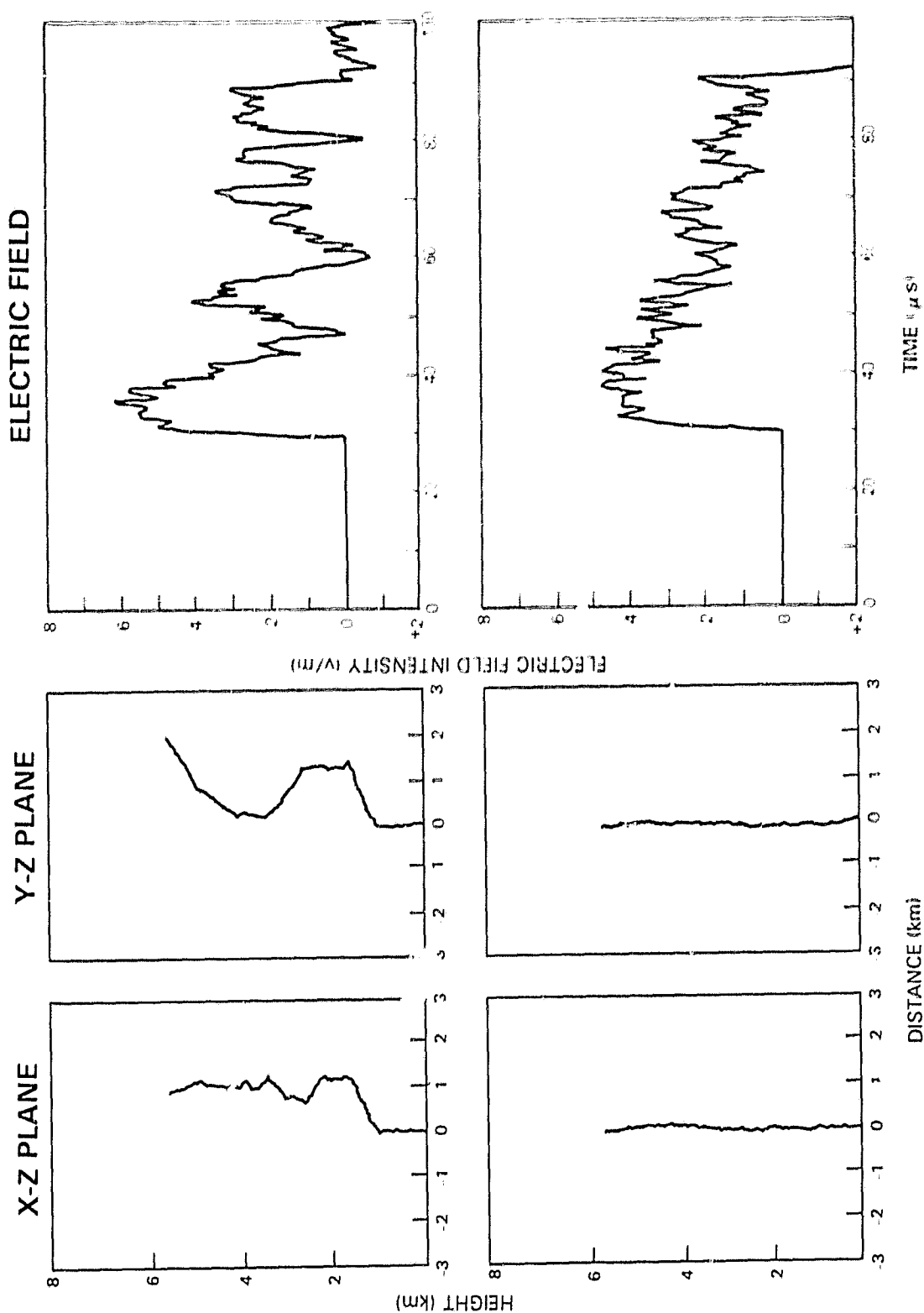


Figure 10. Electric field waveforms (right) radiated from the channels shown at the left. The channels have been generated with the same statistics except that the channel at the top has large scale fluctuations whereas the channel at the bottom does not.

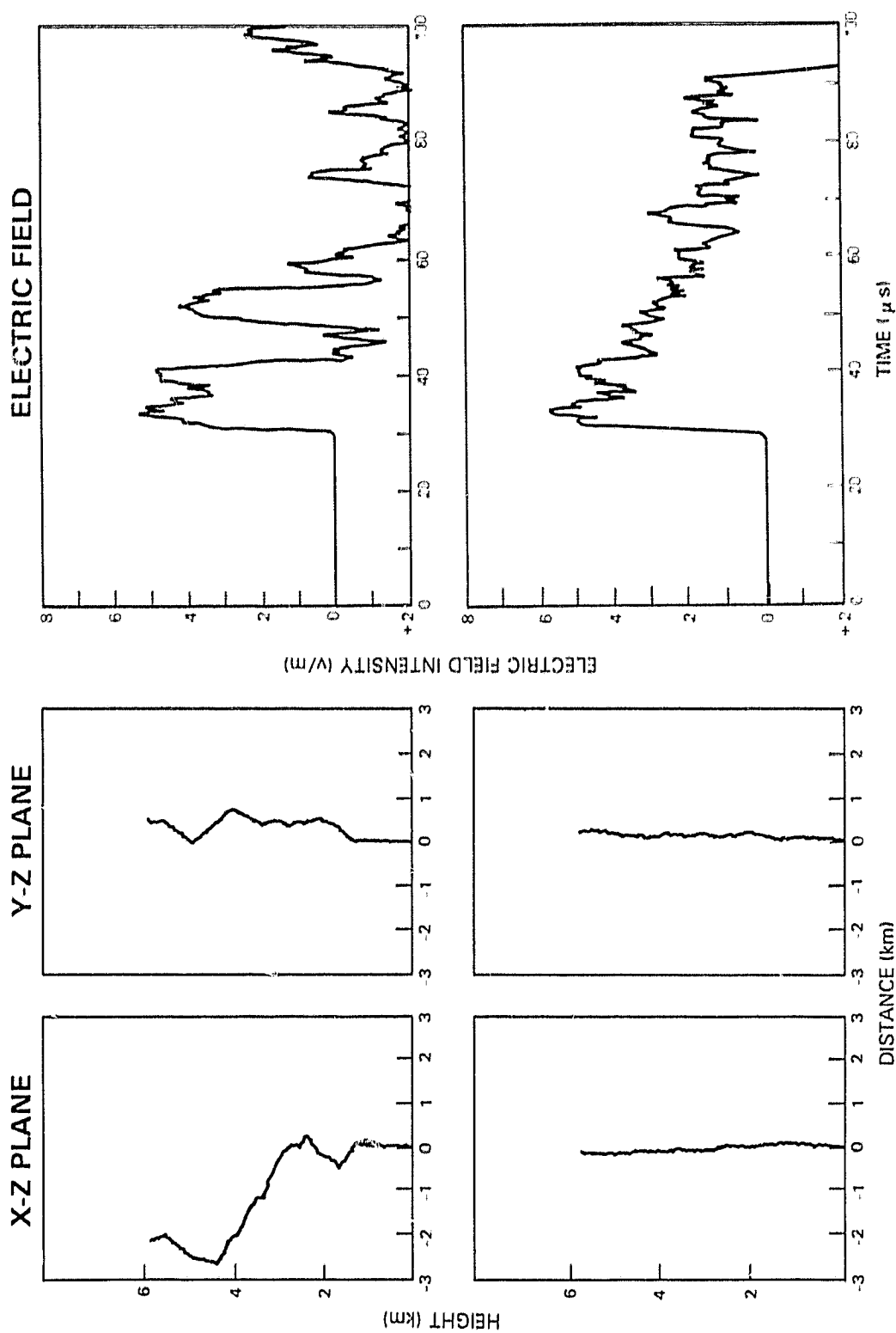


Figure 11. Electric field waveforms (right) radiated from the channels shown at the left. The two channels have been generated with the same statistics except that the channel at the top includes large scale fluctuations whereas the example at the bottom does not.

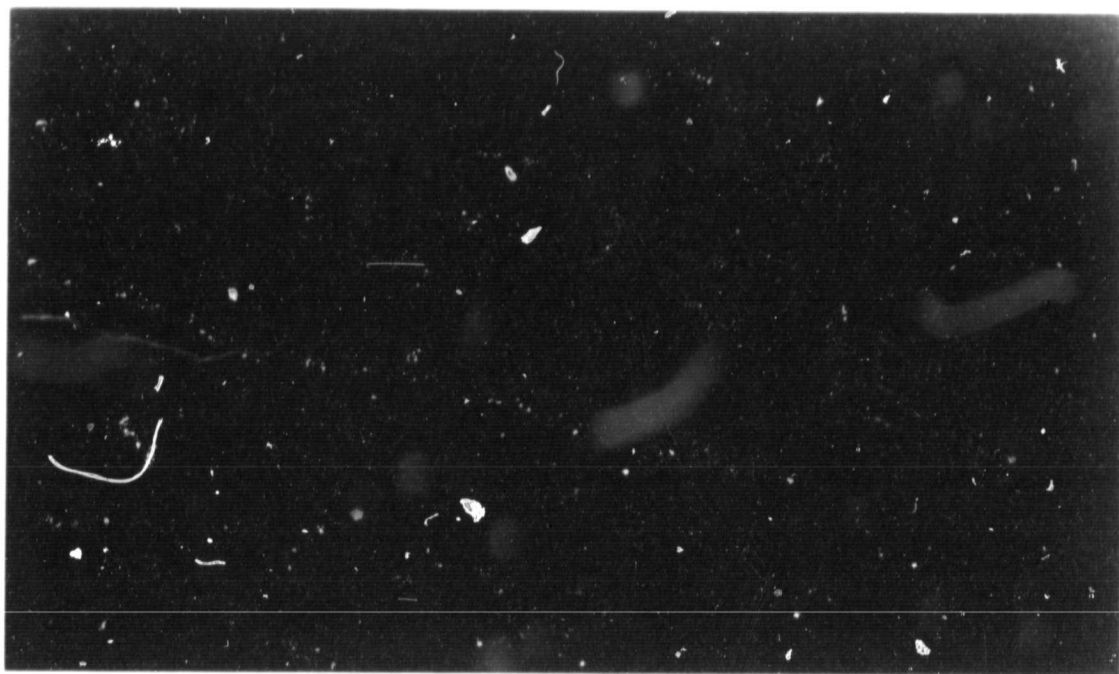
APPENDIX A

Lightning Photographs

Prints of the original lightning photographs from which channels A-H were selected for analysis are shown in this appendix. The letter above each print corresponds to the letter assigned to the channels. In cases where more than one return stroke channel is present in the photograph, the image with the best optical quality was selected. For example, in Flashes A, B and D the channels on the far left were chosen for analysis.

ORIGINAL PAGE IS
OF POOR QUALITY

B



A

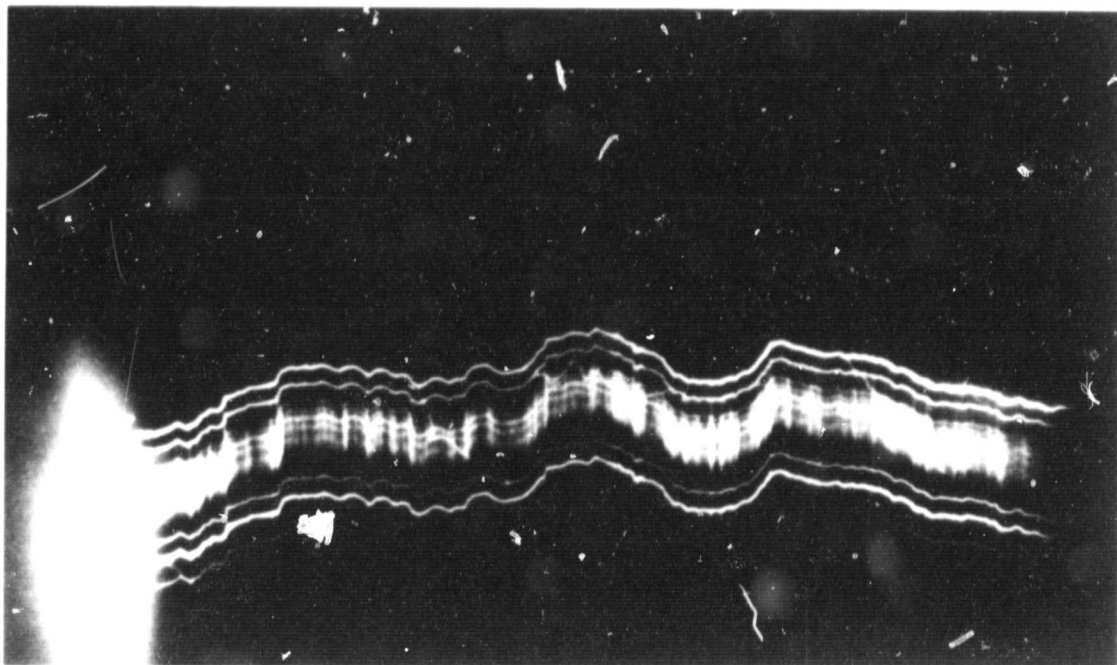


Figure A1. Lightning flashes A and B.

ORIGINAL PAGE IS
OF POOR QUALITY

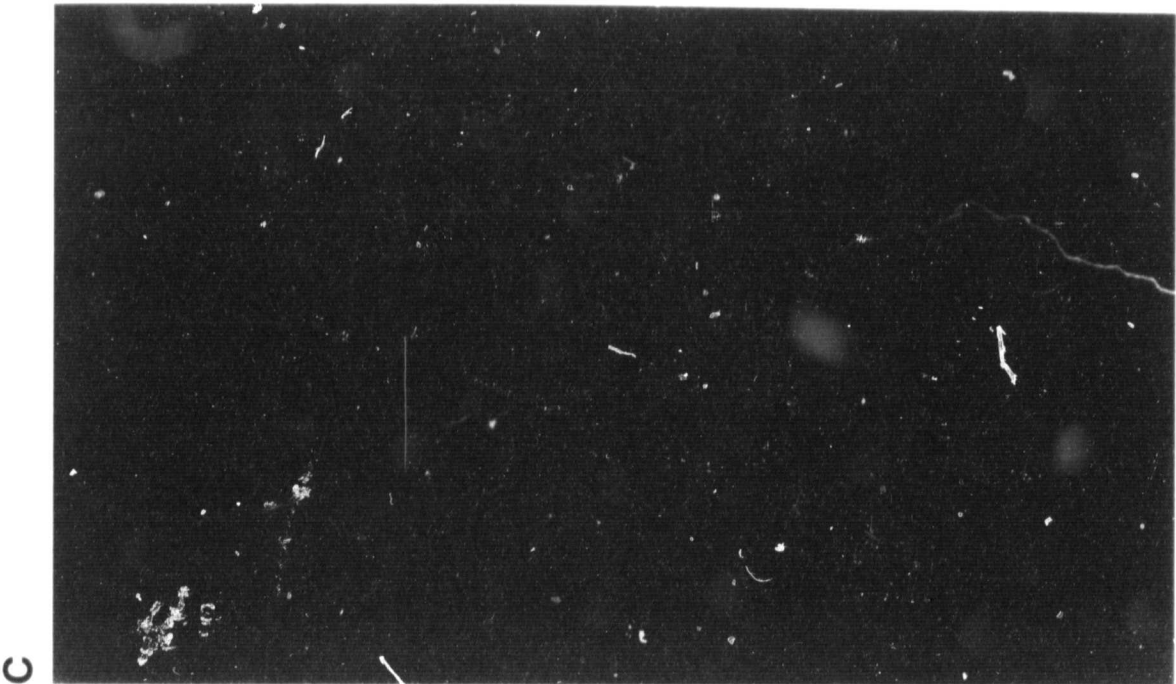
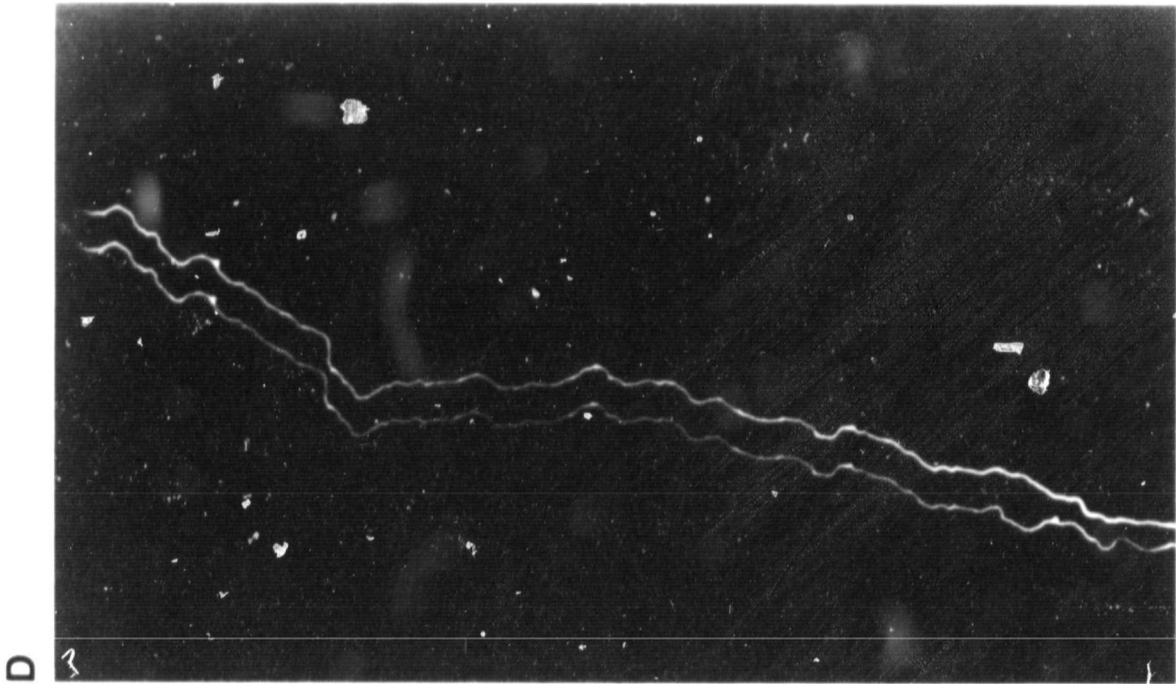
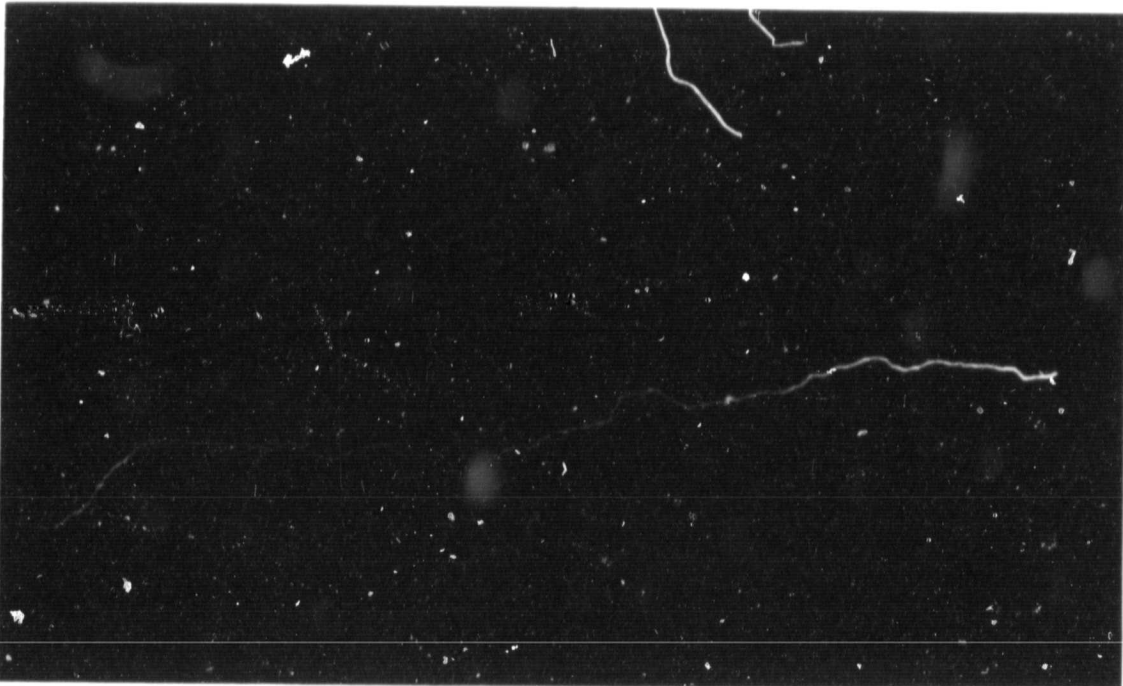


Figure A2. Lightning flashes C and D.

F



E

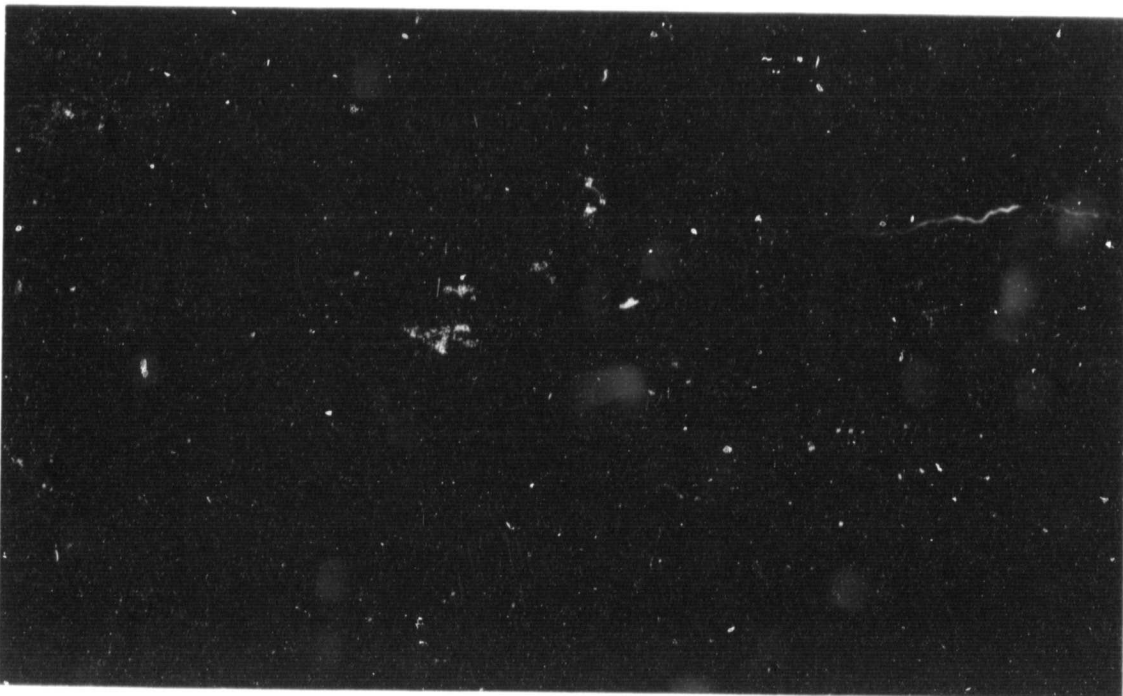
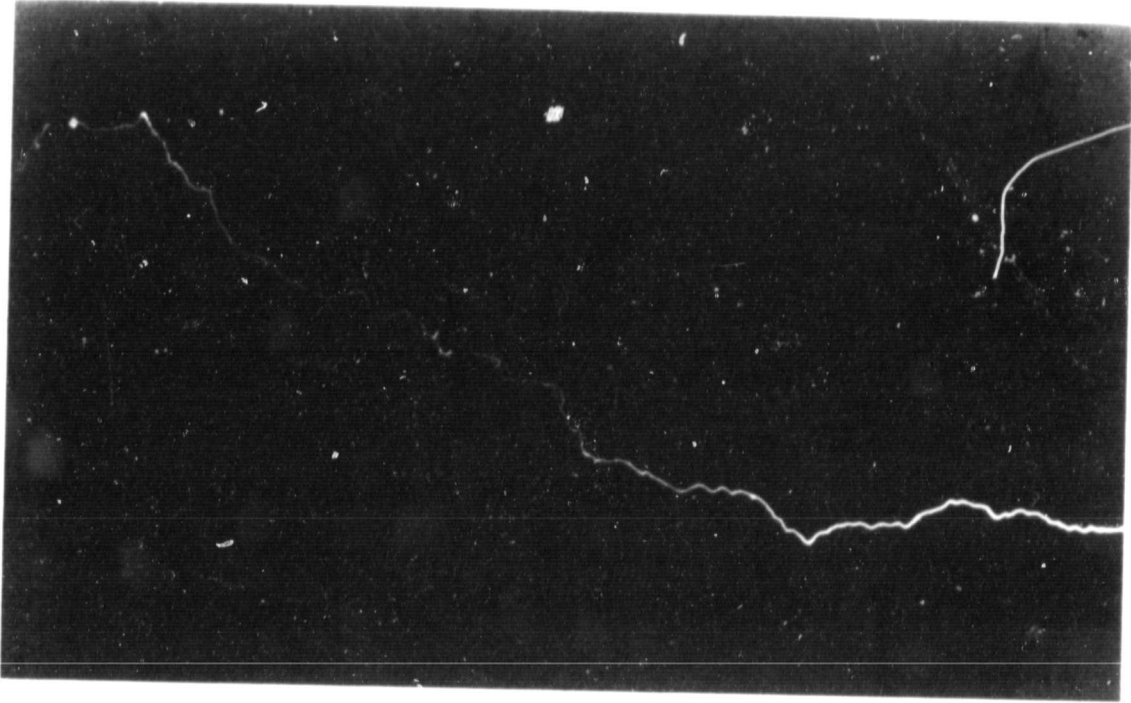


Figure A3. Lightning flashes E and F.

ORIGINAL PAGE IS
OF POOR QUALITY

H



G

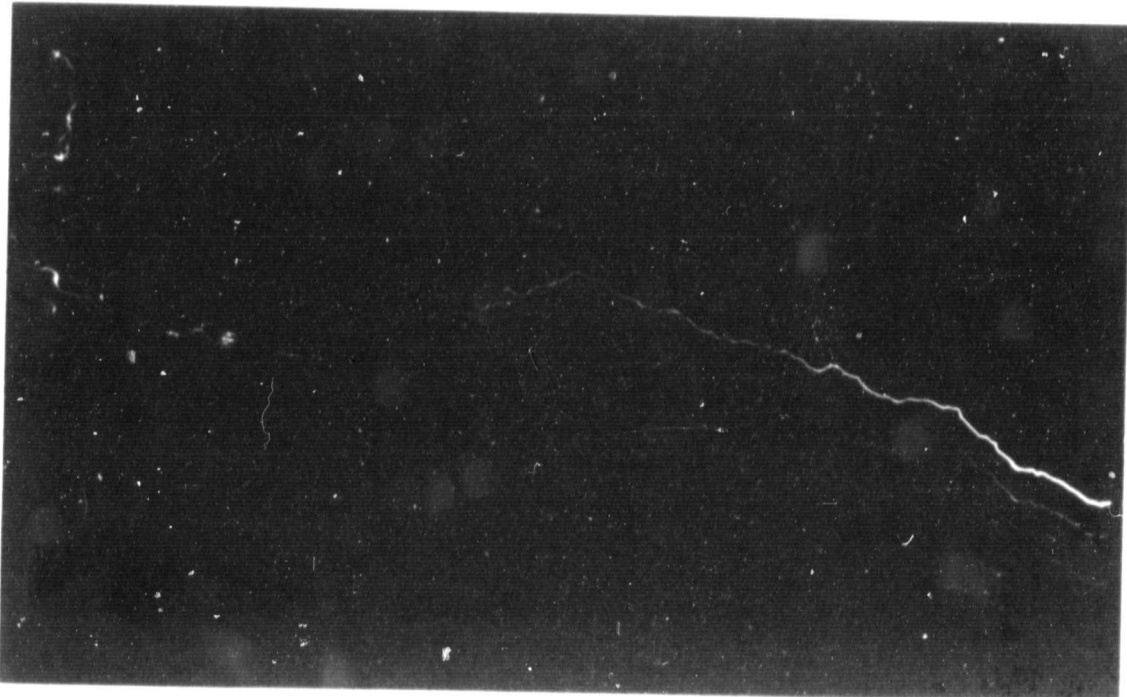


Figure A4. Lightning flashes G and H.

APPENDIX B

List of Data Points

Listed in this appendix are the differences ΔX and ΔZ of the cartesian coordinates between ends of the linear segments used to fit lightning channels A - H (Figures 1-4). The piecewise linear fit was made by following the channel with a straightedge until the edge departed from the channel by about one channel width. The straightedge was then re-oriented to follow the channel. ΔX and ΔZ are the change in cartesian coordinate between ends of these segments. ΔZ is the change in the vertical direction and ΔX is the change in the horizontal direction. The data points as listed are in arbitrary units equal to the number of grid lines crossed in going from one end of the segment to the other. The grid was superimposed on top of the channel. The conversion to meters is as described in the text.

PRECEDING PAGE BLANK NOT FILMED

Channel A
Horizontal Changes ΔZ

1	1	58	-3	115	-2	172	-1
2	-2	59	-5	116	0	173	2
3	3	60	5	117	-1	174	-1
4	2	61	0	118	-2	175	-2
5	5	62	1	119	-1	176	2
6	0	63	-1	120	-2	177	-2
7	4	64	-4	121	1	178	0
8	0	65	-1	122	1	179	-1
9	-1	66	1	123	0	180	-1
10	4	67	0	124	-3	181	-1
11	1	68	-2	125	0	182	0
12	-1	69	-5	126	-1	183	-2
13	1	70	-1	127	-1	184	1
14	-1	71	-1	128	-2	185	-2
15	1	72	-1	129	-1	186	1
16	2	73	7	130	-2	187	-1
17	1	74	0	131	-3	188	-5
18	5	75	-3	132	-10	189	0
19	12	76	0	133	0	190	-1
20	0	77	3	134	-5	191	-1
21	12	78	0	135	1	192	-3
22	0	79	-1	136	0	193	-1
23	3	80	1	137	-1	194	-3
24	2	81	2	138	-2	195	-2
25	2	82	4	139	2	196	0
26	2	83	4	140	-1	197	-2
27	3	84	1	141	-1	198	0
28	3	85	2	142	1	199	-2
29	1	86	0	143	0	200	-1
30	1	87	-4	144	-1	201	1
31	11	88	-2	145	1	202	-1
32	0	89	-1	146	2	203	-1
33	4	90	-1	147	0	204	1
34	6	91	1	148	2	205	-2
35	1	92	1	149	-1	206	0
36	5	93	2	150	2	207	2
37	0	94	1	151	1	208	0
38	2	95	4	152	3	209	-3
39	1	96	4	153	0	210	-3
40	0	97	4	154	4	211	0
41	1	98	4	155	2	212	-1
42	0	99	2	156	3	213	-2
43	9	100	3	157	3	214	0
44	3	101	3	158	2	215	-5
45	0	102	0	159	4	216	0
46	2	103	1	160	0	217	2
47	-1	104	1	161	1	218	0
48	1	105	4	162	1	219	-5
49	-2	106	0	163	-1	220	-0
50	2	107	-3	164	0	221	-1
51	0	108	-1	165	-2	222	-3
52	2	109	-4	166	-2	223	-1
53	-1	110	0	167	-1	224	1
54	-3	111	-3	168	-1	225	0
55	0	112	1	169	-2	226	-1
56	2	113	1	170	1		
57	1	114	-5	171	-3		

ORIGINAL PAGE IS
OF POOR QUALITY

Channel A
Vertical Changes ΔX

1	2	58	8	115	2	172	10
2	4	59	5	116	4	173	8
3	4	60	5	117	2	174	3
4	1	61	5	118	0	175	3
5	1	62	3	119	-1	176	8
6	2	63	3	120	2	177	2
7	2	64	3	121	2	178	2
8	4	65	4	122	2	179	4
9	2	66	2	123	1	180	2
10	5	67	7	124	2	181	3
11	5	68	3	125	4	182	4
12	3	69	1	126	2	183	2
13	3	70	2	127	3	184	4
14	3	71	1	128	3	185	3
15	3	72	4	129	2	186	2
16	3	73	11	130	3	187	3
17	8	74	5	131	1	188	4
18	5	75	9	132	7	189	3
19	5	76	2	133	5	190	2
20	2	77	2	134	8	191	2
21	-2	78	4	135	2	192	3
22	2	79	3	136	2	193	4
23	1	80	2	137	3	194	3
24	6	81	2	138	2	195	0
25	0	82	0	139	3	196	7
26	3	83	5	140	6	197	4
27	5	84	5	141	1	198	1
28	2	85	5	142	3	199	2
29	0	86	3	143	4	200	1
30	2	87	3	144	2	201	4
31	2	88	2	145	1	202	4
32	2	89	3	146	2	203	6
33	5	90	5	147	5	204	5
34	0	91	4	148	1	205	3
35	4	92	6	149	4	206	5
36	10	93	5	150	2	207	1
37	2	94	3	151	3	208	3
38	5	95	3	152	3	209	3
39	8	96	5	153	5	210	11
40	5	97	2	154	2	211	4
41	0	98	6	155	3	212	2
42	4	99	1	156	2	213	1
43	3	100	1	157	1	214	4
44	3	101	1	158	3	215	5
45	2	102	5	159	1	216	10
46	1	103	3	160	4	217	4
47	3	104	5	161	3	218	3
48	3	105	7	162	2	219	4
49	3	106	11	163	2	220	3
50	4	107	3	164	3	221	1
51	10	108	1	165	1	222	7
52	6	109	7	166	1	223	4
53	5	110	3	167	7	224	6
54	9	111	4	168	2	225	8
55	3	112	2	169	1	226	2
56	3	113	2	170	3	227	4
57	7	114	5	171	4		

ORIGINAL PAGE IS
OF POOR QUALITY

Channel B
Horizontal Changes ΔX

1	4	68	4	135	3	202	3
2	8	69	3	136	5	203	1
3	5	70	1	137	3	204	3
4	3	71	1	138	2	205	2
5	4	72	4	139	3	206	0
6	3	73	1	140	6	207	-2
7	4	74	4	141	-	208	2
8	12	75	3	142	4	209	3
9	2	76	3	143	4	210	4
10	2	77	4	144	4	211	5
11	2	78	4	145	3	212	4
12	11	79	5	146	3	213	2
13	5	80	3	147	4	214	3
14	3	81	2	148	4	215	2
15	4	82	5	149	7	216	3
16	3	83	3	150	4	217	0
17	3	84	2	151	3	218	3
18	4	85	4	152	3	219	2
19	1	86	2	153	3	220	3
20	5	87	4	154	3	221	0
21	17	88	4	155	4	222	4
22	3	89	2	156	4	223	5
23	-8	90	2	157	5	224	8
24	8	91	2	158	3	225	3
25	5	92	7	159	2	226	2
26	8	93	3	160	2	227	3
27	5	94	4	161	4	228	3
28	3	95	2	162	1	229	5
29	4	96	9	163	3	230	5
30	5	97	3	164	4	231	1
31	4	98	4	165	8	232	3
32	5	99	3	166	-1	233	2
33	4	100	4	167	9	234	2
34	4	101	5	168	8	235	2
35	5	102	3	169	2	236	3
36	3	103	4	170	2	237	7
37	7	104	1	171	3	238	3
38	7	105	1	172	3	239	2
39	5	106	5	173	3	240	3
40	3	107	1	174	3	241	3
41	4	108	5	175	2	242	3
42	5	109	3	176	3	243	3
43	2	110	3	177	1	244	2
44	3	111	4	178	3	245	4
45	8	112	2	179	4	246	2
46	9	113	4	180	7	247	2
47	5	114	2	181	1	248	7
48	5	115	2	182	4	249	3
49	3	116	3	183	11	250	4
50	7	117	2	184	3	251	3
51	9	118	3	185	1	252	2
52	10	119	1	186	2	253	4
53	8	120	3	187	3	254	7
54	5	121	3	188	6	255	6
55	6	122	5	189	4	256	6
56	5	123	5	190	7	257	9
57	2	124	2	191	1	258	4
58	7	125	2	192	3	259	4
59	3	126	1	193	4	260	3
60	3	127	5	194	5	261	3
61	3	128	3	195	6	262	1
62	4	129	1	196	4	263	5
63	11	130	1	197	9	264	3
64	7	131	1	198	6	265	1
65	4	132	1	199	2	266	-1
66	3	133	2	200	3		
67	3	134	1	201	2		

ORIGINAL DATA IS
OF POOR QUALITY

Channel B
Vertical Changes ΔZ

1	-2	69	-1	136	1	203	2
2	0	70	0	137	1	204	0
3	-1	71	4	138	0	205	0
4	2	72	3	139	-2	206	0
5	-2	73	1	140	-1	207	1
6	0	74	1	141	-1	208	1
7	2	75	1	142	0	209	2
8	-2	76	5	143	1	210	1
9	1	77	1	144	1	211	0
10	1	78	0	145	-1	212	4
11	2	79	-1	146	0	213	0
12	4	80	-1	147	1	214	2
13	3	81	0	148	-1	215	0
14	0	82	4	149	0	216	2
15	-1	83	0	150	-1	217	2
16	0	84	-1	151	0	218	2
17	1	85	0	152	-3	219	3
18	3	86	1	153	1	220	2
19	2	87	0	154	1	221	1
20	2	88	2	155	1	222	0
21	-3	89	0	156	1	223	3
22	0	90	0	157	2	224	4
23	1	91	2	158	1	225	3
24	0	92	2	159	1	226	2
25	1	93	3	160	-1	227	-1
26	2	94	1	161	-1	228	0
27	0	95	1	162	2	229	3
28	3	96	0	163	0	230	-1
29	-1	97	-1	164	1	231	-3
30	0	98	6	165	2	232	0
31	2	99	1	166	2	233	-3
32	1	100	1	167	6	234	0
33	1	101	0	168	1	235	2
34	2	102	-1	169	-1	236	0
35	0	103	1	170	-5	237	-2
36	3	104	1	171	5	238	-1
37	1	105	3	172	3	239	0
39	-2	106	3	173	-1	240	1
40	0	107	1	174	-2	241	0
41	-1	108	3	175	0	242	0
42	-2	109	-1	176	1	243	1
43	-3	110	0	177	3	244	0
44	1	111	2	178	0	245	-1
45	-2	112	2	179	0	246	1
46	-1	113	2	180	2	247	3
47	2	114	0	181	1	248	0
48	0	115	-3	182	2	249	-1
49	-1	116	0	183	1	250	0
50	-1	117	1	184	-6	251	2
51	-1	118	0	185	16	252	3
52	-8	119	-1	186	0	253	2
53	-2	120	-3	187	2	254	3
54	0	121	4	188	1	256	4
55	3	122	-1	189	-1	257	4
56	0	123	1	190	1	258	5
57	-2	124	2	191	2	259	3
58	-4	125	-4	192	0	260	5
59	1	126	0	193	-3	261	0
60	2	127	-2	194	0	262	-3
61	0	128	-1	195	1	263	0
62	3	129	1	196	-2	264	-1
63	0	130	1	197	-1	265	-2
64	-3	131	2	198	-3	266	-3
65	-1	132	3	199	-7		
66	-4	133	3	200	-3		
67	-1	134	4	201	1		
68	0	135	3	202	1		

ORIGINAL PAGE IS
OF POOR QUALITY

Channel C
Horizontal Changes ΔX

1	2.00	62	3.00	123	1.50	184	-3.00
2	1.00	63	1.00	124	-1.50	185	-2.50
3	3.00	64	1.00	125	2.00	186	3.00
4	2.00	65	0.50	126	-0.50	187	-7.00
5	5.00	66	-0.50	127	-2.00	188	0.00
6	3.00	67	0.50	128	-1.50	189	-5.00
7	1.00	68	2.00	129	0.50	190	-0.50
8	0.50	69	5.00	130	-1.00	191	-1.00
9	1.00	70	-4.00	131	0.00	192	-3.00
10	1.00	71	-2.50	132	-0.50	193	-2.00
11	5.00	72	-0.50	133	-3.00	194	-2.50
12	1.00	73	0.50	134	0.50	195	-2.00
13	-1.00	74	0.00	135	-0.50	196	-4.00
14	1.50	75	-3.50	136	1.00	197	-2.00
15	2.50	76	-3.00	137	-0.50	198	-1.00
16	4.00	77	-4.50	138	-0.50	199	0.50
17	0.00	78	-3.00	139	-2.00	200	-2.00
18	0.50	79	-1.50	140	-0.50	201	-1.00
19	1.00	80	-3.00	141	-2.50	202	-2.00
20	2.00	81	-2.50	142	-0.50	203	-1.50
21	9.00	82	-4.00	143	-1.00	204	1.00
22	4.50	83	2.50	144	-2.00	205	-1.00
23	3.00	84	-1.50	145	-3.00	206	0.50
24	3.50	85	-4.00	146	-2.00	207	2.00
25	3.00	86	-3.50	147	0.00	208	0.00
26	3.00	87	-1.00	148	-2.00	209	0.00
27	2.00	88	-1.00	149	-2.00	210	-1.50
28	2.00	89	-8.00	150	-8.50	211	-5.50
29	2.00	90	-1.00	151	0.50	212	-1.00
30	2.00	91	-1.80	152	3.00	213	-2.50
31	0.50	92	-2.00	153	7.00	214	-1.00
32	-1.00	93	-0.50	154	2.50	215	-2.50
33	-1.00	94	-3.00	155	7.00	216	-2.00
34	-0.50	95	-1.00	156	4.00	217	1.00
35	0.50	96	-0.50	157	5.00	218	5.00
36	3.50	97	-4.50	158	1.00	219	3.00
37	2.00	98	-0.50	159	1.00	220	-1.00
38	1.00	99	-2.00	160	0.50	221	-1.00
39	2.00	100	-3.50	161	-0.50	222	0.50
40	2.50	101	-3.50	162	-8.00	223	2.00
41	1.50	102	-2.50	163	-3.00	224	-1.00
42	1.00	103	-3.00	164	-7.50	225	1.00
43	0.00	104	-13.00	165	-5.00	226	0.00
44	-1.00	105	-5.00	166	-4.00	227	-1.50
45	-2.50	106	-2.00	167	0.00	228	-3.00
46	-4.00	107	-4.00	168	-2.00	229	-0.50
47	-3.00	108	-4.00	169	1.00	230	0.50
48	-1.50	109	-3.50	170	-4.50	231	6.00
49	-3.00	110	-1.50	171	-0.50	232	0.00
50	-1.50	111	-3.00	172	1.00	233	1.50
51	-1.50	112	-3.00	173	-1.00	234	5.00
52	-1.00	113	-2.00	174	-5.50	235	3.00
53	-4.00	114	-3.00	175	-6.00	236	1.50
54	-3.50	115	-5.50	176	-1.00	237	2.00
55	-0.50	116	-3.00	177	-3.00	238	2.00
56	-1.00	117	1.00	178	-4.00	239	3.00
57	-2.00	118	-1.00	179	1.00	240	5.00
58	0.50	119	-5.50	180	0.00	241	1.00
59	-0.50	120	-4.00	181	-4.00	242	4.00
60	-2.50	121	-0.50	182	0.50	243	1.00
61	-0.00	122	-0.00	183	-12.00	244	-1.50

ORIGINAL PAGE IS
OF POOR QUALITY

Channel C
Vertical Changes ΔZ

1	8.00	62	4.50	123	5.50	184	5.50
2	6.00	63	4.00	124	6.50	185	7.50
3	9.00	64	3.00	125	7.00	186	6.00
4	3.00	65	2.00	126	15.00	187	8.50
5	3.00	66	6.00	127	2.00	188	5.50
6	11.00	67	3.50	128	7.50	189	4.50
7	5.00	68	4.00	129	3.00	190	2.50
8	4.00	69	3.50	130	4.50	191	2.00
9	3.00	70	4.00	131	10.50	192	3.00
10	2.00	71	4.00	132	2.50	193	5.50
11	5.50	72	1.50	133	1.00	194	12.00
12	3.00	73	4.00	134	5.00	195	2.00
13	9.00	74	2.00	135	2.50	196	3.00
14	10.00	75	9.00	136	9.00	197	2.00
15	6.00	76	0.00	137	2.50	198	2.50
16	8.50	77	-0.50	138	5.00	199	8.00
17	2.50	78	-0.50	139	1.00	200	4.00
18	5.50	79	2.00	140	3.00	201	4.00
19	2.00	80	3.00	141	3.00	202	3.00
20	2.50	81	0.50	142	4.00	203	4.00
21	5.50	82	1.50	143	1.50	204	5.50
22	3.50	83	1.50	144	1.00	205	1.50
23	3.00	84	1.50	145	0.50	206	3.50
24	4.00	85	6.00	146	1.50	207	3.00
25	6.00	86	1.50	147	2.50	208	3.00
26	8.00	87	1.00	148	4.00	209	6.00
27	2.00	88	2.50	149	2.00	210	3.50
28	1.50	89	4.50	150	3.50	211	5.50
29	1.50	90	2.00	151	1.50	212	3.00
30	9.00	91	7.50	152	2.00	213	16.50
31	2.00	92	23.00	153	1.00	214	2.00
32	3.50	93	1.50	154	2.00	215	3.50
33	1.00	94	2.50	155	3.50	216	1.50
34	2.00	95	2.00	156	-2.00	217	2.00
35	3.00	96	2.00	157	1.00	218	5.00
36	6.00	97	10.00	158	2.00	219	6.50
37	2.00	98	2.00	159	2.00	220	6.00
38	1.50	99	3.50	160	2.00	221	5.00
39	2.50	100	0.50	161	3.50	222	5.00
40	7.00	101	1.50	162	6.00	223	6.00
41	4.00	102	3.00	163	3.00	224	9.00
42	3.50	103	8.00	164	-4.50	225	6.50
43	6.50	104	12.50	165	2.00	226	1.50
44	3.00	105	-1.00	166	8.50	227	3.00
45	1.00	106	0.50	167	1.50	228	3.00
46	-3.00	107	1.50	168	3.00	229	6.00
47	0.50	108	3.00	169	3.00	230	1.50
48	8.50	109	5.50	170	7.50	231	7.00
49	4.00	110	1.50	171	2.00	232	3.50
50	3.00	111	0.50	172	2.50	233	2.50
51	5.50	112	2.00	173	2.00	234	3.00
52	2.50	113	4.50	174	1.50	235	3.00
53	5.00	114	3.00	175	4.00	236	7.50
54	4.50	115	4.50	176	1.50	237	7.50
55	3.00	116	4.50	177	4.50	238	2.50
56	6.00	117	4.00	178	5.00	239	2.00
57	8.50	118	11.50	179	5.00	240	1.00
58	7.00	119	7.50	180	4.00	241	1.50
59	2.00	120	7.00	181	7.00	242	5.00
60	5.50	121	2.00	182	4.00	243	5.00
61	4.00	122	1.00	183	12.00	244	9.00

Channel D
Horizontal Changes ΔX

ORIGINAL DATES
OF POOR QUALITY

1	1.00	55	3.50	109	-1.00	163	1.50
2	-2.50	56	2.00	110	-2.00	164	3.00
3	-2.00	57	0.50	111	-3.50	165	3.50
4	-0.50	58	2.00	112	-4.00	166	2.00
5	0.00	59	3.00	113	-4.00	167	1.00
6	1.50	60	0.00	114	-1.50	168	3.00
7	7.00	61	2.00	115	-0.50	169	2.00
8	0.00	62	4.50	116	0.50	170	2.50
9	-1.50	63	-1.00	117	0.50	171	7.00
10	-4.00	64	0.50	118	1.00	172	1.00
11	-3.00	65	-6.00	119	-0.50	173	1.50
12	-0.50	66	-2.50	120	-4.00	174	3.50
13	2.00	67	-1.00	121	0.50	175	4.00
14	5.00	68	-0.50	122	-2.00	176	1.00
15	2.00	69	1.00	123	1.00	177	0.00
16	1.00	70	2.00	124	4.50	178	0.50
17	2.50	71	3.50	125	4.00	179	1.00
18	5.00	72	6.50	126	2.00	180	3.00
19	4.00	73	1.50	127	-0.50	181	3.00
20	1.00	74	-2.00	128	-2.00	182	3.00
21	-1.00	75	0.50	129	-3.50	183	4.00
22	-0.50	76	-0.50	130	-1.50	184	2.00
23	0.50	77	2.00	131	-0.50	185	3.00
24	3.00	78	2.50	132	-0.50	186	2.50
25	-1.50	79	1.50	133	-3.00	187	0.50
26	-0.50	80	1.50	134	1.00	188	-1.00
27	0.50	81	8.50	135	3.50	189	-1.00
28	-3.00	82	1.00	136	0.50	190	-3.00
29	-3.50	83	-2.00	137	-4.00	191	-1.50
30	-1.50	84	-1.50	138	1.50	192	-0.50
31	-1.00	85	-0.50	139	-3.00	193	0.50
32	2.00	86	1.00	140	-0.50	194	13.00
33	3.00	87	3.50	141	-3.50	195	2.50
34	1.50	88	3.00	142	-5.00	196	5.00
35	1.00	89	3.50	143	-2.00	197	2.00
36	1.00	90	3.00	144	-0.50	198	1.00
37	3.00	91	2.50	145	0.00	199	0.00
38	5.00	92	0.50	146	1.50	200	1.00
39	2.00	93	0.50	147	3.50	201	2.00
40	0.00	94	1.00	148	2.50	202	1.00
41	-4.00	95	-2.50	149	5.50	203	1.00
42	1.00	96	0.50	150	7.00	204	3.00
43	1.00	97	1.50	151	2.00	205	5.00
44	-0.50	98	-1.00	152	1.50	206	3.00
45	2.00	99	-2.00	153	1.50	207	2.00
46	-1.00	100	-0.50	154	5.00	208	1.00
47	-0.50	101	-0.50	155	9.00	209	4.00
48	3.00	102	2.50	156	8.00	210	2.00
49	2.00	103	2.00	157	2.50	211	-5.50
50	2.00	104	5.50	158	3.50	212	-1.50
51	2.50	105	2.50	159	3.00	213	-0.50
52	-1.00	106	2.00	160	2.00	214	1.50
53	1.00	107	-1.00	161	1.00	215	1.00
54	5.00	108	-1.00	162	1.00		

Channel D
Vertical Changes ΔZ

1	5.00	55	5.50	109	6.00	163	2.00
2	6.50	56	6.00	110	2.50	164	2.00
3	5.50	57	5.00	111	3.00	165	4.50
4	2.50	58	8.00	112	9.00	166	4.00
5	9.00	59	7.00	113	6.00	167	4.00
6	3.50	60	5.50	114	4.50	168	6.00
7	12.00	61	3.50	115	6.00	169	6.00
8	7.50	62	4.00	116	4.00	170	2.50
9	2.50	63	4.00	117	3.50	171	5.00
10	2.00	64	4.00	118	6.00	172	3.00
11	5.00	65	5.00	119	3.50	173	3.50
12	4.00	66	3.50	120	10.00	174	7.00
13	3.00	67	5.50	121	5.00	175	2.00
14	3.00	68	4.50	122	8.00	176	3.00
15	3.00	69	4.00	123	5.00	177	5.50
16	6.00	70	2.00	124	0.50	178	3.50
17	3.00	71	3.50	125	5.50	179	2.00
18	3.50	72	11.50	126	6.00	180	2.50
19	4.50	73	15.50	127	3.00	181	5.00
20	5.00	74	7.50	128	5.00	182	2.00
21	4.00	75	10.50	129	6.50	183	1.00
22	2.50	76	6.00	130	5.00	184	1.50
23	3.50	77	7.00	131	9.00	185	4.00
24	4.00	78	4.50	132	4.00	186	5.00
25	1.50	79	2.50	133	12.00	187	3.50
26	3.50	80	3.50	134	2.50	188	4.00
27	4.00	81	13.00	135	3.50	189	4.90
28	3.00	82	5.50	136	2.00	190	3.00
29	2.50	83	9.50	137	8.00	191	3.50
30	3.00	84	4.50	138	13.00	192	3.50
31	6.00	85	5.00	139	3.50	193	3.50
32	5.00	86	2.50	140	6.00	194	15.00
33	5.00	87	3.00	141	3.50	195	2.00
34	3.00	88	2.50	142	8.00	196	0.50
35	2.00	89	4.50	143	6.00	197	2.00
36	3.00	90	3.00	144	3.00	198	3.00
37	4.00	91	2.50	145	2.50	199	4.50
38	2.00	92	3.50	146	2.00	200	2.00
39	3.50	93	2.50	147	1.00	201	1.50
40	2.00	94	4.00	148	1.50	202	4.50
41	15.50	95	6.00	149	10.00	203	3.00
42	7.00	96	3.00	150	3.00	204	2.00
43	19.50	97	7.00	151	2.50	205	2.00
44	6.00	98	4.00	152	5.00	206	2.00
45	5.00	99	4.00	153	1.50	207	3.00
46	6.00	100	6.50	154	2.00	208	3.00
47	5.00	101	7.50	155	0.50	209	3.00
48	6.00	102	2.50	156	-0.50	210	4.90
49	3.00	103	9.00	157	1.50	211	8.00
50	2.00	104	2.00	158	3.50	212	2.70
51	5.50	105	3.00	159	7.00	213	3.50
52	5.50	106	5.00	160	6.00	214	12.00
53	2.00	107	4.00	161	7.00	215	2.50
54	5.00	108	3.00	162	3.00		

Channel E
Horizontal Changes ΔX

1	0.00	64	2.00	127	-2.00	190	-1.00
2	4.00	65	3.00	128	-1.00	191	-3.00
3	2.50	66	0.00	129	-2.00	192	-0.50
4	3.50	67	-2.00	130	-6.50	193	-1.00
5	2.00	68	1.00	131	-2.00	194	-1.00
6	3.00	69	-7.00	132	-2.00	195	-3.00
7	-1.00	70	0.00	133	-4.00	196	0.00
8	-2.00	71	-4.00	134	-4.00	197	1.50
9	1.00	72	0.00	135	-5.00	198	0.00
10	0.00	73	-1.00	136	-5.50	199	-0.50
11	-2.00	74	-4.00	137	-3.00	200	-5.50
12	-0.50	75	-1.00	138	-7.00	201	-4.00
13	5.00	76	-4.00	139	-3.00	202	-0.50
14	-0.30	77	4.00	140	-2.50	203	4.00
15	1.00	78	2.00	141	-4.00	204	0.00
16	-1.00	79	9.00	142	-4.00	205	2.00
17	-6.00	80	2.50	143	-1.50	206	0.50
18	-4.00	81	6.00	144	-5.00	207	0.50
19	0.30	82	2.00	145	-5.00	208	4.00
20	-1.00	83	-1.00	146	-3.00	209	5.00
21	-3.00	84	-2.00	147	-9.00	210	3.00
22	0.00	85	-2.00	148	-3.00	211	-1.00
23	-3.50	86	-3.00	149	-2.00	212	-2.00
24	-7.50	87	1.00	150	-11.50	213	-1.00
25	-1.00	88	3.50	151	-2.00	214	-2.00
26	0.00	89	3.00	152	-2.00	215	-4.00
27	2.50	90	0.00	153	-3.00	216	-1.00
28	-1.00	91	-3.00	154	-2.00	217	-4.00
29	1.00	92	-1.00	155	-2.00	218	1.00
30	0.50	93	-1.00	156	-2.00	219	0.00
31	-0.50	94	-4.00	157	-4.00	220	-2.00
32	-4.00	95	-1.00	158	0.00	221	-7.00
33	-2.00	96	-2.00	159	-2.00	222	-3.00
34	0.00	97	-0.50	160	-2.00	223	-3.00
35	-7.00	98	-4.00	161	-1.50	224	-5.00
36	-3.00	99	0.00	162	-0.50	225	-5.50
37	-3.00	100	1.00	163	-0.30	226	-3.50
38	-2.00	101	-3.00	164	-4.00	227	-2.00
39	-2.00	102	0.00	165	-2.00	228	-2.00
40	-4.00	103	-1.00	166	-1.00	229	-8.00
41	1.50	104	-3.00	167	-1.00	230	-2.00
42	-2.00	105	-2.50	168	-2.00	231	-7.00
43	-1.00	106	-4.00	169	1.00	232	-2.00
44	1.00	107	-3.00	170	-0.50	233	-13.00
45	-0.50	108	-6.00	171	-1.00	234	-3.00
46	1.00	109	-3.00	172	-7.00	235	-9.00
47	-0.50	110	-5.00	173	-3.00	236	-1.00
48	1.00	111	-10.00	174	-1.00	237	-2.00
49	1.00	112	-3.00	175	-1.00	238	-4.00
50	-2.50	113	3.00	176	-6.00	239	-14.00
51	-4.00	114	-1.00	177	-2.00	240	-2.00
52	-1.50	115	-1.50	178	3.00	241	-3.50
53	-2.00	116	-3.00	179	0.00	242	-3.00
54	-5.00	117	-2.00	180	-1.00	243	-2.00
55	-3.50	118	-2.00	181	-2.00	244	-6.00
56	-1.00	119	-1.00	182	-6.00	245	-6.00
57	0.00	120	-2.00	183	1.00	246	-7.00
58	0.00	121	-3.00	184	0.00	247	-0.50
59	-1.00	122	-4.00	185	-1.00	248	0.30
60	-1.00	123	-2.00	186	-1.00	249	7.00
61	-2.00	124	-2.00	187	-5.00	250	1.00
62	-1.00	125	-9.00	188	1.00	251	-0.50
63	2.50	126	-3.00	189	-0.50	252	-2.00

Channel E
OF POOR QUALITY

Channel E
Vertical Changes ΔZ

1	6.50	64	6.00	127	4.00	190	2.50
2	0.00	65	5.00	128	1.00	191	6.50
3	2.50	66	4.00	129	1.00	192	2.00
4	7.50	67	6.50	130	1.00	193	2.00
5	6.00	68	8.00	131	1.00	194	2.50
6	11.00	69	14.00	132	2.00	195	5.00
7	4.50	70	12.00	133	6.00	196	1.50
8	2.50	71	6.00	134	3.00	197	3.00
9	6.00	72	8.00	135	2.00	198	5.50
10	3.00	73	2.00	136	0.50	199	3.00
11	6.00	74	2.00	137	0.00	200	4.50
12	10.00	75	2.00	138	-2.50	201	4.00
13	11.00	76	12.00	139	2.00	202	8.50
14	5.00	77	10.00	140	2.50	203	4.00
15	9.50	78	2.00	141	5.00	204	5.00
16	6.00	79	4.00	142	5.00	205	3.00
17	20.00	80	2.50	143	0.50	206	2.50
18	3.00	81	7.00	144	1.00	207	6.50
19	5.00	82	5.00	145	1.00	208	7.50
20	3.00	83	11.00	146	1.00	209	6.00
21	4.00	84	4.00	147	3.50	210	9.00
22	4.00	85	3.00	148	0.50	211	1.50
23	3.50	86	4.00	149	0.00	212	1.50
24	4.50	87	2.00	150	-1.00	213	2.50
25	2.00	88	4.50	151	0.00	214	1.50
26	4.00	89	5.00	152	1.00	215	1.00
27	6.00	90	6.00	153	2.00	216	2.00
28	6.00	91	6.00	154	3.00	217	4.00
29	3.00	92	3.50	155	1.50	218	5.00
30	1.00	93	5.00	156	1.00	219	2.00
31	2.00	94	3.00	157	8.00	220	2.00
32	11.00	95	1.00	158	15.00	221	5.00
33	3.00	96	6.00	159	0.00	222	2.00
34	6.00	97	3.00	160	2.00	223	1.00
35	13.50	98	7.00	161	4.00	224	0.00
36	4.00	99	17.00	162	3.00	225	2.50
37	6.00	100	9.00	163	1.00	226	2.00
38	4.50	101	7.50	164	1.00	227	6.00
39	15.00	102	7.00	165	-1.00	228	4.00
40	6.00	103	4.00	166	4.00	229	-0.50
41	8.00	104	3.50	167	2.00	230	-1.00
42	3.00	105	2.00	168	1.50	231	-8.00
43	2.00	106	1.00	169	3.00	232	-2.00
44	7.00	107	3.00	170	2.00	233	3.00
45	8.00	108	0.50	171	1.00	234	0.00
46	6.00	109	0.50	172	1.00	235	-10.00
47	7.00	110	7.00	173	1.50	236	-2.00
48	4.00	111	3.00	174	3.00	237	-1.00
49	4.00	112	3.00	175	3.50	238	1.00
50	9.00	113	3.50	176	5.00	239	2.50
51	8.50	114	7.50	177	2.00	240	1.50
52	3.50	115	2.50	178	9.00	241	2.00
53	7.00	116	3.50	179	3.00	242	0.00
54	4.00	117	0.00	180	5.00	243	0.50
55	6.00	118	1.50	181	5.00	244	4.00
56	4.00	119	9.50	182	12.00	245	3.00
57	6.00	120	4.00	183	5.00	246	10.00
58	4.00	121	2.00	184	2.50	247	3.00
59	5.00	122	1.00	185	2.00	248	1.50
60	3.00	123	2.00	186	2.00	249	11.00
61	3.00	124	1.00	187	6.00	250	3.00
62	8.00	125	1.00	188	6.00	251	4.00
63	8.50	126	1.00	189	2.00	252	4.00

Channel F
Horizontal Changes ΔX

ORIGINAL PAGE IS
OF POOR QUALITY

1	-3.50	54	0.00	106	-5.00	158	-1.00
2	-1.00	55	-3.00	107	-3.50	159	-3.50
3	-4.00	56	0.00	108	-1.50	160	-1.00
4	-1.50	57	0.00	109	-1.00	161	-0.50
5	-0.50	58	-0.50	110	-0.50	162	1.00
6	4.00	59	-2.00	111	0.00	163	-2.00
7	4.00	60	-2.50	112	-3.00	164	1.50
8	0.50	61	-2.00	113	-3.50	165	1.00
9	-1.00	62	-9.00	114	-5.00	166	0.00
10	0.50	63	-0.50	115	-2.00	167	-2.00
11	-1.00	64	1.00	116	-17.00	168	-3.00
12	-1.50	65	4.00	117	-2.00	169	2.00
13	-0.50	66	-8.00	118	-1.00	170	0.50
14	1.00	67	-1.00	119	-0.50	171	0.00
15	0.00	68	0.00	120	0.50	172	0.50
16	-1.00	69	1.00	121	1.50	173	0.00
17	-0.50	70	-0.50	122	0.00	174	-2.50
18	-0.50	71	-1.50	123	-2.00	175	-0.50
19	-2.50	72	-1.00	124	0.00	176	-0.50
20	-3.00	73	-1.00	125	1.00	177	-0.50
21	-1.70	74	-3.00	126	5.00	178	0.00
22	-0.80	75	-4.00	127	2.00	179	1.00
23	-1.00	76	2.00	128	4.00	180	-5.00
24	-3.00	77	5.00	129	-5.50	181	-2.00
25	-0.50	78	3.00	130	4.00	182	-0.50
26	1.50	79	1.00	131	1.00	183	-0.50
27	0.50	80	2.50	132	1.00	184	1.00
28	-0.50	81	0.50	133	6.00	185	-2.50
29	7.00	82	-0.50	134	1.00	186	-1.50
30	0.50	83	-6.00	135	0.00	187	-1.50
31	-2.50	84	0.50	136	-1.00	188	-9.00
32	-0.50	85	-1.00	137	-1.50	189	-7.00
33	-5.00	86	-2.00	138	-2.00	190	-3.00
34	-3.00	87	-2.00	139	-2.50	191	-2.00
35	-2.00	88	-5.50	140	-1.00	192	-5.00
36	-0.50	89	-3.00	141	-0.50	193	-3.00
37	-1.50	90	-6.00	142	-1.50	194	-3.00
38	-2.00	91	-2.00	143	-2.50	195	-2.00
39	-4.50	92	-7.00	144	-5.50	196	-7.00
40	-2.00	93	-2.50	145	-1.00	197	-1.00
41	-2.00	94	-4.00	146	0.00	198	-1.00
42	-1.50	95	-6.50	147	-1.00	199	-4.00
43	-0.50	96	-0.50	148	-1.00	200	-6.50
44	0.00	97	-1.00	149	0.00	201	-8.50
45	-1.50	98	-3.00	150	2.00	202	-3.00
46	-5.50	99	-1.00	151	1.00	203	-5.00
47	-2.50	100	0.00	152	1.00	204	-6.00
48	-2.00	101	0.00	153	1.50	205	-3.00
49	-1.50	102	-2.00	154	4.00	206	-5.00
50	-1.00	103	-4.50	155	1.00	207	-3.00
51	-2.00	104	-2.00	156	0.00	208	-3.00
52	-4.00	105	-2.00	157	-1.00	209	-4.50
53	-1.00						

Channel F
Vertical Changes ΔZ

1	5.50	54	6.00	106	2.00	158	2.00
2	2.50	55	6.00	107	2.50	159	3.50
3	14.00	56	3.50	108	2.50	160	3.00
4	6.00	57	3.50	109	2.50	161	4.00
5	4.00	58	2.00	110	3.00	162	13.00
6	6.00	59	5.50	111	7.50	163	6.80
7	6.00	60	6.50	112	12.00	164	6.00
8	3.00	61	4.50	113	2.50	165	3.00
9	13.00	62	9.00	114	5.50	166	2.00
10	9.00	63	2.00	115	5.00	167	6.50
11	13.50	64	2.00	116	12.00	168	4.00
12	10.00	65	4.00	117	2.50	169	10.00
13	4.00	66	1.50	118	2.00	170	2.50
14	4.00	67	1.00	119	3.00	171	4.00
15	3.00	68	3.50	120	6.00	172	5.50
16	6.00	69	5.00	121	5.50	173	3.50
17	12.50	70	2.00	122	3.00	174	6.50
18	9.00	71	2.00	123	8.50	175	2.00
19	4.00	72	2.50	124	3.00	176	6.00
20	3.00	73	9.00	125	2.00	177	3.50
21	2.50	74	4.00	126	6.00	178	5.00
22	1.70	75	10.00	127	3.00	179	7.00
23	5.00	76	3.50	128	11.00	180	7.50
24	6.50	77	13.00	129	14.00	181	4.50
25	4.00	78	8.00	130	6.50	182	2.50
26	7.00	79	2.80	131	6.50	183	3.00
27	1.50	80	3.50	132	2.00	184	9.00
28	3.00	81	7.00	133	7.00	185	8.50
29	8.00	82	2.00	134	2.00	186	2.50
30	3.00	83	5.00	135	1.50	187	1.50
31	15.00	84	4.00	136	13.00	188	6.50
32	2.00	85	5.00	137	3.00	189	6.00
33	7.00	86	8.00	138	1.50	190	4.50
34	5.00	87	6.50	139	2.00	191	2.50
35	4.00	88	1.00	140	3.00	192	4.00
36	2.00	89	1.00	141	3.50	193	1.50
37	9.80	90	3.00	142	7.50	194	1.50
38	2.80	91	0.50	143	3.00	195	3.00
39	3.00	92	0.50	144	4.50	196	2.00
40	2.50	93	1.00	145	1.50	197	1.50
41	5.00	94	9.50	146	3.50	198	3.50
42	6.00	95	17.50	147	4.50	199	2.00
43	3.50	96	5.50	148	3.00	200	3.00
44	2.50	97	3.00	149	3.00	201	3.00
45	1.50	98	5.00	150	7.50	202	3.50
46	3.50	99	3.00	151	3.00	203	2.50
47	2.00	100	5.50	152	7.50	204	11.00
48	2.50	101	3.00	153	6.00	205	3.00
49	4.00	102	2.50	154	9.00	206	3.00
50	2.50	103	6.00	155	3.00	207	2.50
51	2.50	104	4.00	156	6.00	208	3.00
52	5.00	105	5.50	157	6.00	209	4.50
53	2.00						

ORIGINAL PAGE IS
OF POOR QUALITY

Channel G
Horizontal Changes ΔX

1	-0.50	53	5.00	105	-3.00	156	-0.50
2	1.50	54	7.50	106	-4.50	157	4.00
3	5.00	55	-1.00	107	-2.00	158	0.00
4	4.50	56	1.50	108	-1.00	159	-0.50
5	6.00	57	4.00	109	-1.00	160	-2.50
6	5.00	58	0.50	110	-2.00	161	0.00
7	5.00	59	3.50	111	-2.00	162	0.00
8	-1.00	60	-1.50	112	-5.00	163	2.00
9	4.00	61	0.00	113	-2.00	164	1.00
10	-0.50	62	0.50	114	-2.00	165	2.00
11	1.00	63	2.00	115	0.50	166	7.00
12	2.00	64	0.00	116	6.00	167	-0.50
13	14.00	65	-1.00	117	-4.00	168	0.00
14	2.50	66	5.50	118	-1.00	169	-4.00
15	2.00	67	2.00	119	-2.00	170	0.00
16	3.00	68	2.00	120	0.00	171	-1.00
17	1.00	69	5.00	121	0.50	172	1.00
18	3.00	70	2.00	122	0.00	173	0.50
19	1.00	71	5.50	123	-1.00	174	2.00
20	2.00	72	3.00	124	-4.00	175	9.00
21	9.00	73	1.00	125	-2.00	176	-2.50
22	10.00	74	-1.00	126	-1.00	177	0.50
23	4.50	75	2.00	127	-0.50	178	7.00
24	0.00	76	2.50	128	-4.00	179	1.50
25	0.50	77	2.00	129	-2.50	180	5.00
26	-0.50	78	3.00	130	-2.00	181	-0.50
27	1.00	79	5.50	131	-0.50	182	-1.50
28	2.00	80	2.00	132	-0.50	183	3.00
29	2.00	81	3.00	133	1.00	184	9.00
30	1.00	82	3.00	134	2.00	185	0.50
31	1.50	83	3.00	135	1.00	186	1.00
32	-0.50	84	2.00	136	-0.50	187	2.50
33	-2.00	85	-1.00	137	-1.00	188	2.00
34	-1.00	86	6.00	138	-2.00	189	2.50
35	5.00	87	0.50	139	-2.50	190	4.50
36	0.50	88	-1.50	140	-6.00	191	5.00
37	1.50	89	-3.50	141	-7.00	192	2.50
38	2.00	90	-1.50	142	-5.00	193	2.00
39	3.00	91	-2.00	143	-1.00	194	2.00
40	4.00	92	-1.50	144	-0.50	195	1.00
41	6.00	93	-1.50	145	0.50	196	0.00
42	2.50	94	-1.00	146	2.00	197	1.00
43	2.00	95	-1.50	147	1.00	198	3.00
44	5.50	96	-3.50	148	2.00	199	13.00
45	1.50	97	-1.00	149	2.00	200	5.00
46	1.00	98	-2.00	150	3.00	201	3.00
47	-3.00	99	-1.00	151	2.00	202	2.00
48	-1.00	100	0.00	152	1.00	203	1.50
49	-0.50	101	1.50	153	4.00	204	2.50
50	0.50	102	3.00	154	0.50	205	4.00
51	1.00	103	3.50	155	-1.00	206	2.50
52	3.50	104	-1.00				

ORIGINAL RECORD
OF POOR QUALITY

Channel G
Vertical Changes ΔZ

1	5.00	53	5.00	105	1.00	156	4.00
2	10.50	54	16.00	106	0.00	157	11.00
3	6.00	55	6.00	107	0.50	158	3.00
4	8.00	56	4.50	108	1.00	159	3.00
5	9.50	57	4.00	109	5.00	160	6.00
6	9.50	58	10.00	110	5.00	161	3.00
7	12.00	59	7.50	111	8.50	162	1.50
8	4.00	60	8.50	112	3.00	163	5.00
9	4.50	61	5.00	113	2.00	164	3.00
10	7.50	62	2.50	114	2.50	165	2.00
11	5.00	63	2.50	115	3.00	166	7.00
12	3.00	64	2.00	116	11.50	167	2.00
13	15.00	65	8.00	117	8.00	168	2.50
14	2.50	66	6.50	118	3.50	169	5.50
15	1.00	67	9.00	119	12.00	170	5.50
16	1.00	68	4.00	120	6.50	171	6.00
17	3.00	69	4.50	121	8.00	172	4.50
18	3.00	70	3.50	122	5.00	173	4.50
19	5.00	71	8.50	123	4.00	174	5.00
20	4.00	72	8.00	124	9.00	175	11.00
21	9.00	73	8.50	125	3.00	176	6.00
22	8.50	74	4.00	126	3.50	177	3.00
23	1.50	75	11.00	127	6.00	178	5.50
24	6.00	76	6.50	128	5.50	179	1.50
25	3.00	77	2.90	129	6.50	180	12.00
26	3.00	78	3.00	130	3.50	181	4.00
27	4.00	79	15.50	131	4.00	182	8.00
28	3.50	80	5.00	132	3.50	183	10.00
29	5.00	81	3.00	133	3.50	184	9.00
30	6.00	82	3.00	134	5.50	185	10.00
31	13.50	83	3.50	135	3.00	186	5.00
32	4.50	84	3.50	136	2.50	187	4.00
33	2.50	85	7.00	137	2.50	188	2.50
34	4.00	86	10.00	138	2.00	189	2.50
35	9.00	87	3.50	139	1.00	190	2.00
36	5.50	88	5.00	140	2.00	191	-0.50
37	5.00	89	4.00	141	10.00	192	0.50
38	4.00	90	4.50	142	6.00	193	1.00
39	4.50	91	4.50	143	2.00	194	4.00
40	4.00	92	3.00	144	4.50	195	3.50
41	3.00	93	7.50	145	2.00	196	4.50
42	11.00	94	3.50	146	6.50	197	5.00
43	3.00	95	3.50	147	7.00	198	10.00
44	4.00	96	6.50	148	4.00	199	8.00
45	2.50	97	1.00	149	9.00	200	-1.00
46	5.00	98	1.00	150	5.50	201	-0.50
47	6.00	99	3.00	151	3.00	202	1.00
48	2.00	100	3.50	152	2.00	203	2.50
49	5.50	101	3.50	153	3.00	204	1.50
50	2.50	102	4.00	154	2.00	205	-2.00
51	3.00	103	5.50	155	5.00	206	-0.50
52	4.50	104	1.50				

Channel H
Horizontal Changes ΔX

1	0.00	66	0.00	131	0.00	196	3.00
2	-2.00	67	1.50	132	2.00	197	2.00
3	-1.00	68	3.50	133	0.50	198	3.00
4	-0.50	69	3.20	134	0.50	199	3.00
5	0.50	70	2.50	135	1.00	200	2.50
6	1.00	71	0.50	136	-2.00	201	5.00
7	-0.50	72	0.00	137	-1.00	202	13.00
8	-2.00	73	10.00	138	2.00	203	4.00
9	-0.50	74	3.00	139	0.00	204	1.50
10	0.30	75	6.50	140	2.00	205	1.00
11	0.50	76	3.50	141	6.30	206	0.70
12	2.00	77	3.00	142	4.00	207	3.50
13	0.00	78	2.50	143	6.00	208	2.00
14	-1.00	79	4.00	144	2.00	209	5.00
15	5.00	80	0.50	145	2.00	210	8.00
16	1.00	81	0.00	146	0.50	211	1.00
17	7.00	82	-0.50	147	-0.50	212	2.00
18	-0.50	83	-1.00	148	-0.50	213	2.00
19	2.00	84	4.00	149	0.00	214	3.50
20	0.80	85	-2.50	150	-1.00	215	9.00
21	-5.50	86	-1.00	151	-0.50	216	4.00
22	1.00	87	2.50	152	2.00	217	2.50
23	-1.00	88	2.50	153	5.50	218	2.50
24	-3.00	89	0.50	154	4.50	219	5.00
25	1.00	90	-1.50	155	4.50	220	3.00
26	8.00	91	-2.90	156	8.50	221	2.50
27	1.00	92	-2.00	157	4.00	222	3.00
28	0.90	93	-1.00	158	1.50	223	4.50
29	1.50	94	10.00	159	1.50	224	1.50
30	1.20	95	3.00	160	6.50	225	0.00
31	0.70	96	1.00	161	-3.00	226	-2.00
32	-1.50	97	2.00	162	-1.50	227	-3.50
33	-0.50	98	1.00	163	-4.50	228	-4.00
34	1.50	99	-0.50	164	-1.00	229	-2.00
35	0.00	100	1.50	165	3.00	230	-0.50
36	-5.00	101	6.00	166	1.00	231	0.50
37	-2.00	102	2.00	167	11.50	232	-0.50
38	-1.50	103	1.50	168	0.20	233	-2.00
39	-1.00	104	-1.00	169	5.50	234	-1.50
40	-1.50	105	1.00	170	1.00	235	0.00
41	-1.00	106	0.00	171	-1.00	236	0.00
42	-1.50	107	3.00	172	-3.50	237	-0.50
43	-7.00	108	2.80	173	0.50	238	0.00
44	-2.50	109	1.00	174	-1.00	239	1.00
45	0.00	110	4.00	175	0.00	240	3.00
46	3.00	111	6.50	176	1.00	241	1.00
47	0.00	112	7.50	177	5.00	242	1.00
48	-1.50	113	1.00	178	0.50	243	-0.50
49	-0.90	114	0.50	179	0.50	244	-1.20
50	0.00	115	1.00	180	2.50	245	-3.00
51	-0.50	116	1.00	181	3.30	246	0.00
52	-0.50	117	1.50	182	-0.50	247	-1.00
53	-1.50	118	3.00	183	2.50	248	-6.00
54	-1.00	119	6.00	184	2.50	249	-5.00
55	0.50	120	3.50	185	3.00	250	-2.00
56	3.00	121	2.00	186	4.00	251	-4.00
57	1.20	122	2.00	187	3.90	252	-4.50
58	0.00	123	1.50	188	2.00	253	-2.00
59	-5.00	124	3.00	189	7.50	254	-3.00
60	-2.00	125	3.00	190	2.00	255	-5.00
61	-2.00	126	4.00	191	2.00	256	-5.00
62	-0.90	127	3.50	192	3.00	257	-1.00
63	-1.50	128	3.50	193	1.00	258	-3.00
64	-7.00	129	2.00	194	5.00	259	-0.50
65	-1.00	130	0.50	195	4.00		

Channel H
Vertical Changes ΔZ

1	6.00	66	2.00	131	5.00	196	2.00
2	5.00	67	2.00	132	9.00	197	1.50
3	4.00	68	2.00	133	5.00	198	3.00
4	3.50	69	4.50	134	3.00	199	2.00
5	11.00	70	4.60	135	3.00	200	0.50
6	8.00	71	2.00	136	3.00	201	1.00
7	1.50	72	3.50	137	4.00	202	5.00
8	2.00	73	6.50	138	5.50	203	0.50
9	2.50	74	4.00	139	5.50	204	2.00
10	2.00	75	5.00	140	2.00	205	3.00
11	2.00	76	2.50	141	2.00	206	9.20
12	4.00	77	4.00	142	1.50	207	5.50
13	3.00	78	7.50	143	1.00	208	1.00
14	4.00	79	9.00	144	15.00	209	1.00
15	12.00	80	2.00	145	12.00	210	8.00
16	4.00	81	2.00	146	2.50	211	1.50
17	13.50	82	2.90	147	4.00	212	4.00
18	7.00	83	2.50	148	6.00	213	2.00
19	5.00	84	8.00	149	2.50	214	1.00
20	2.00	85	7.00	150	3.00	215	4.00
21	12.00	86	3.00	151	3.00	216	1.80
22	3.50	87	6.00	152	3.50	217	2.50
23	3.00	88	4.50	153	2.00	218	1.50
24	5.50	89	2.50	154	2.90	219	5.00
25	2.00	90	4.00	155	7.50	220	2.00
26	6.00	91	4.20	156	5.00	221	1.50
27	2.00	92	3.50	157	2.50	222	2.50
28	8.50	93	5.00	158	2.50	223	2.50
29	5.50	94	19.50	159	5.00	224	1.50
30	3.50	95	4.00	160	6.50	225	2.50
31	3.50	96	2.00	161	8.00	226	1.00
32	2.50	97	2.00	162	1.90	227	0.50
33	1.50	98	2.50	163	5.00	228	2.00
34	4.00	99	2.50	164	2.00	229	1.50
35	2.00	100	5.00	165	13.50	230	3.00
36	7.00	101	7.20	166	1.00	231	5.00
37	4.00	102	4.80	167	0.00	232	1.00
38	3.00	103	5.50	168	1.00	233	6.00
39	3.00	104	8.80	169	6.00	234	5.00
40	6.00	105	5.00	170	3.00	235	6.00
41	2.00	106	5.00	171	6.50	236	3.00
42	2.00	107	4.80	172	10.00	237	5.00
43	7.00	108	3.80	173	5.00	238	2.50
44	3.50	109	2.50	174	3.00	239	4.50
45	1.00	110	3.00	175	3.00	240	5.00
46	7.00	111	1.00	176	7.50	241	4.00
47	1.50	112	0.00	177	7.50	242	2.00
48	3.50	113	1.00	178	2.00	243	2.50
49	4.00	114	2.00	179	3.00	244	8.00
50	6.50	115	5.00	180	3.50	246	9.00
51	2.00	116	2.00	181	3.00	247	1.50
52	2.00	117	1.50	182	6.00	248	4.00
53	2.20	118	1.00	183	3.00	249	4.00
54	2.00	119	0.00	184	4.00	250	0.50
55	2.00	120	3.50	185	4.00	251	-1.50
56	5.00	121	2.20	186	2.00	252	2.50
57	3.50	122	1.00	187	2.00	253	4.50
58	4.50	123	0.00	188	3.50	254	1.00
59	17.00	124	-0.50	189	22.50	255	1.00
60	5.00	125	-0.50	190	5.00	256	1.00
61	2.00	126	0.90	191	2.00	257	1.50
62	4.90	127	1.00	192	1.00	258	2.00
63	3.00	128	2.50	193	3.00	259	2.50
64	6.30	129	2.00	194	3.00		
65	1.00	130	1.50	195	2.50		

APPENDIX C

HISTOGRAMS FOR THE INDIVIDUAL CHANNELS

Histograms are presented in this appendix for the difference in cartesian coordinates between the ends of the linear segments used to obtain the piecewise linear fit to the channel. The scale on the abscissa in each figure is in relative units. Distance in meters is obtained by multiplying by a scale factor which is determined by the channel length as explained in the text. This scale factor is approximately 2.0 for this data. Two histograms are presented for each channel: one for the change in horizontal coordinate ΔX and one for the change in vertical coordinate ΔZ . The channels themselves are shown in Figures 1-4 and also in appendix A.

PRECEDING PAGE BLANK NOT FILMED

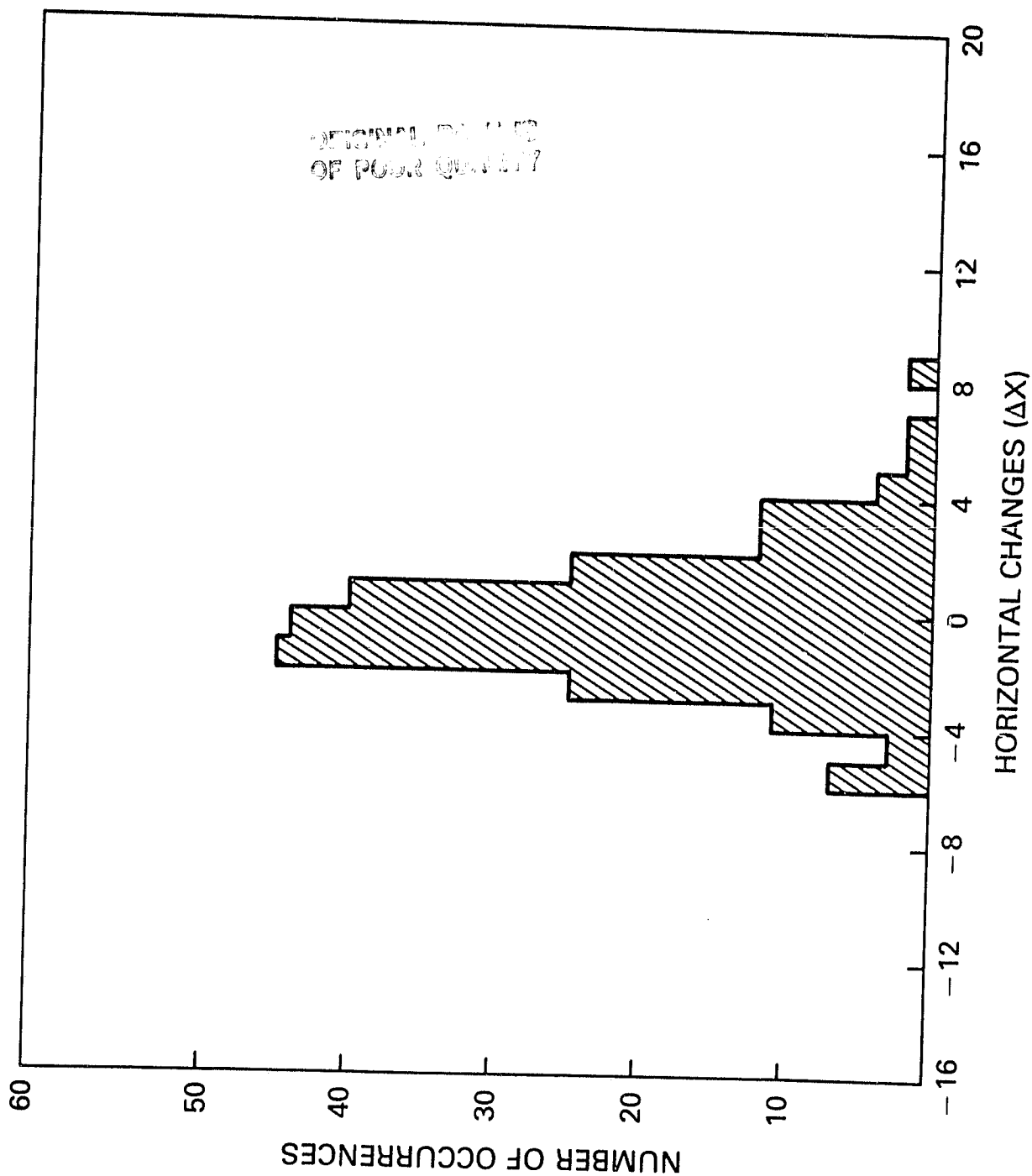


Figure C1. Changes in the horizontal coordinate for channel A.

ORIGINAL PAGE IS
OF POOR QUALITY

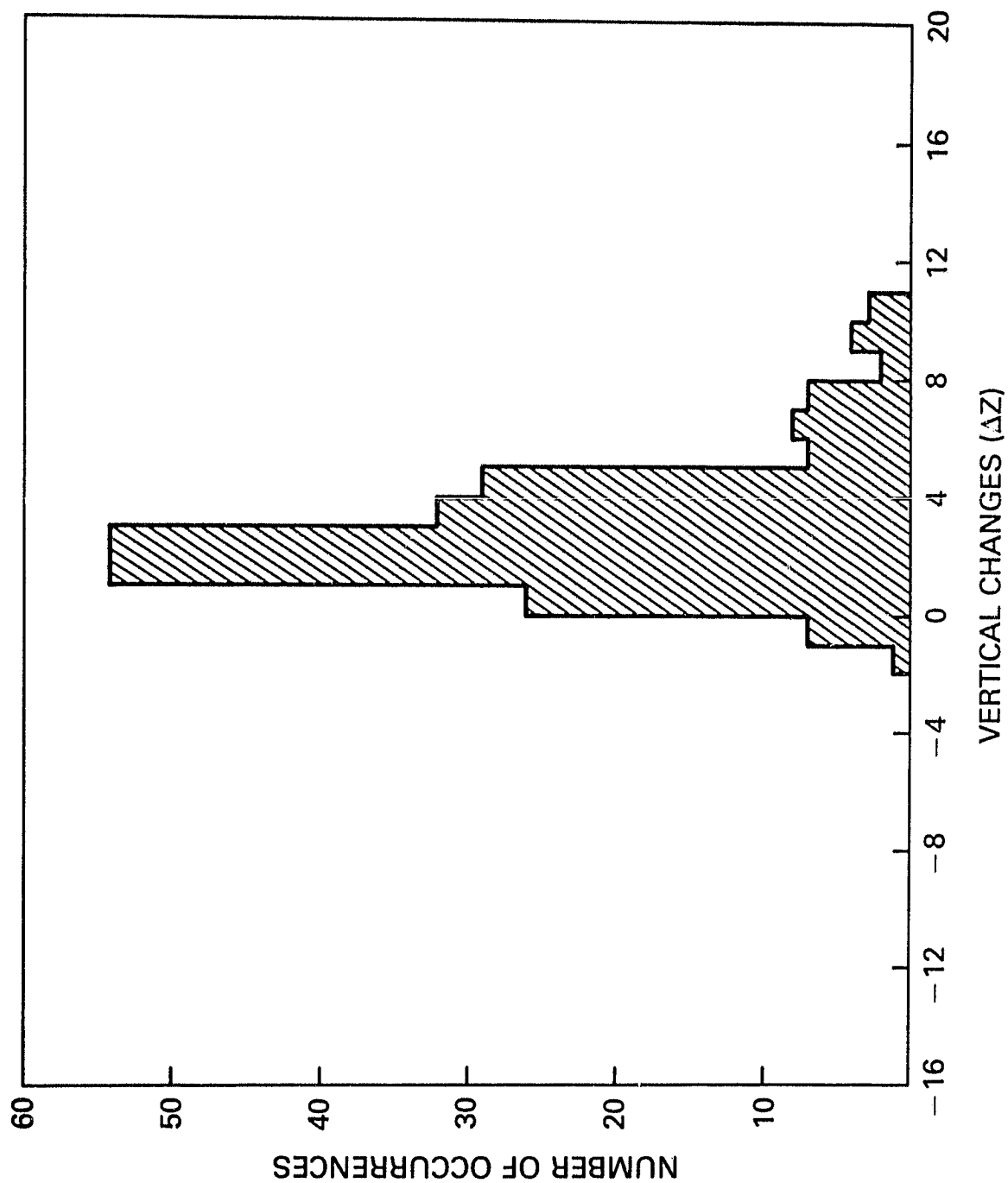


Figure C2. Changes in the vertical coordinate for channel A.

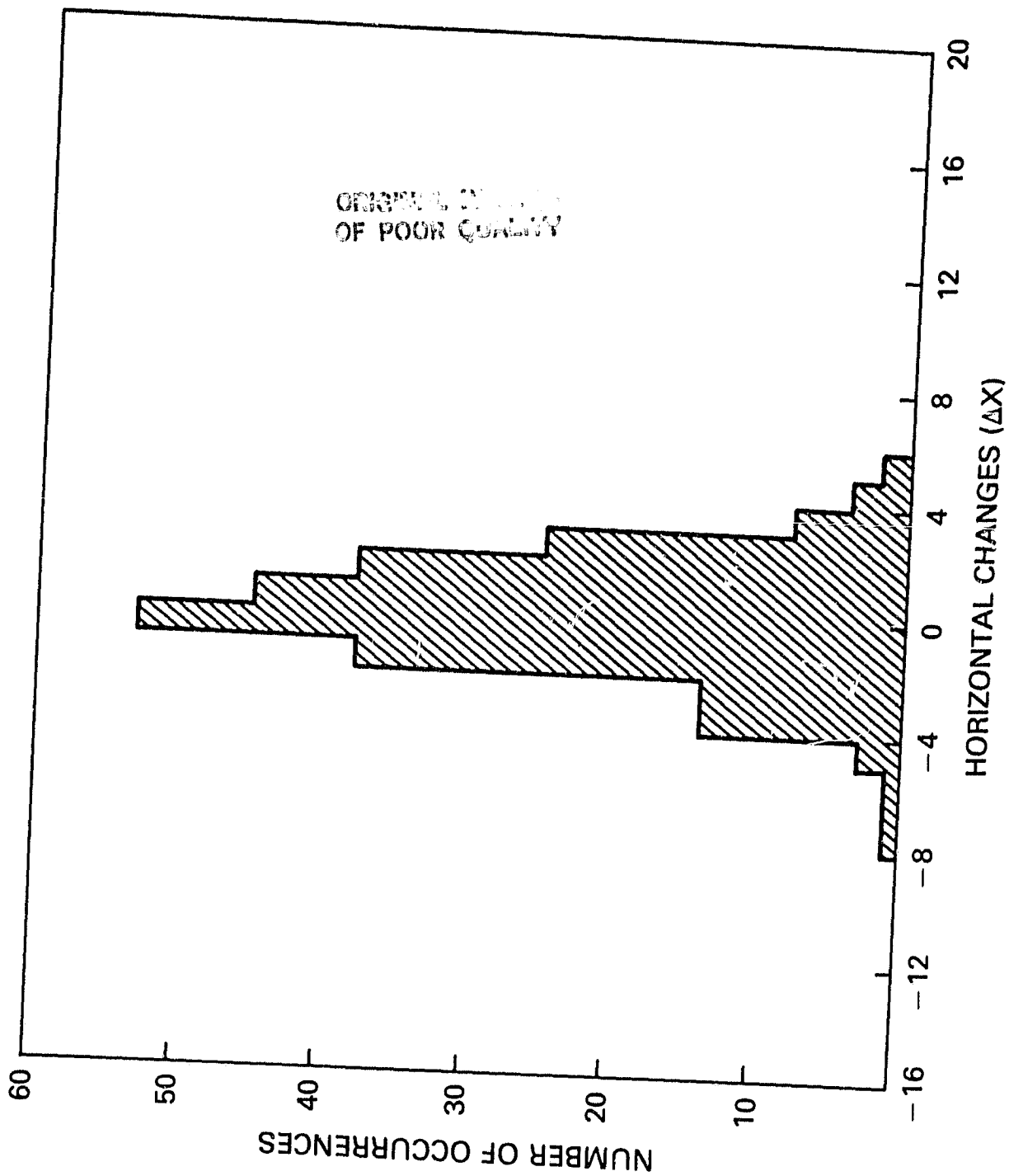


Figure C3. Changes in the horizontal coordinate for channel B.

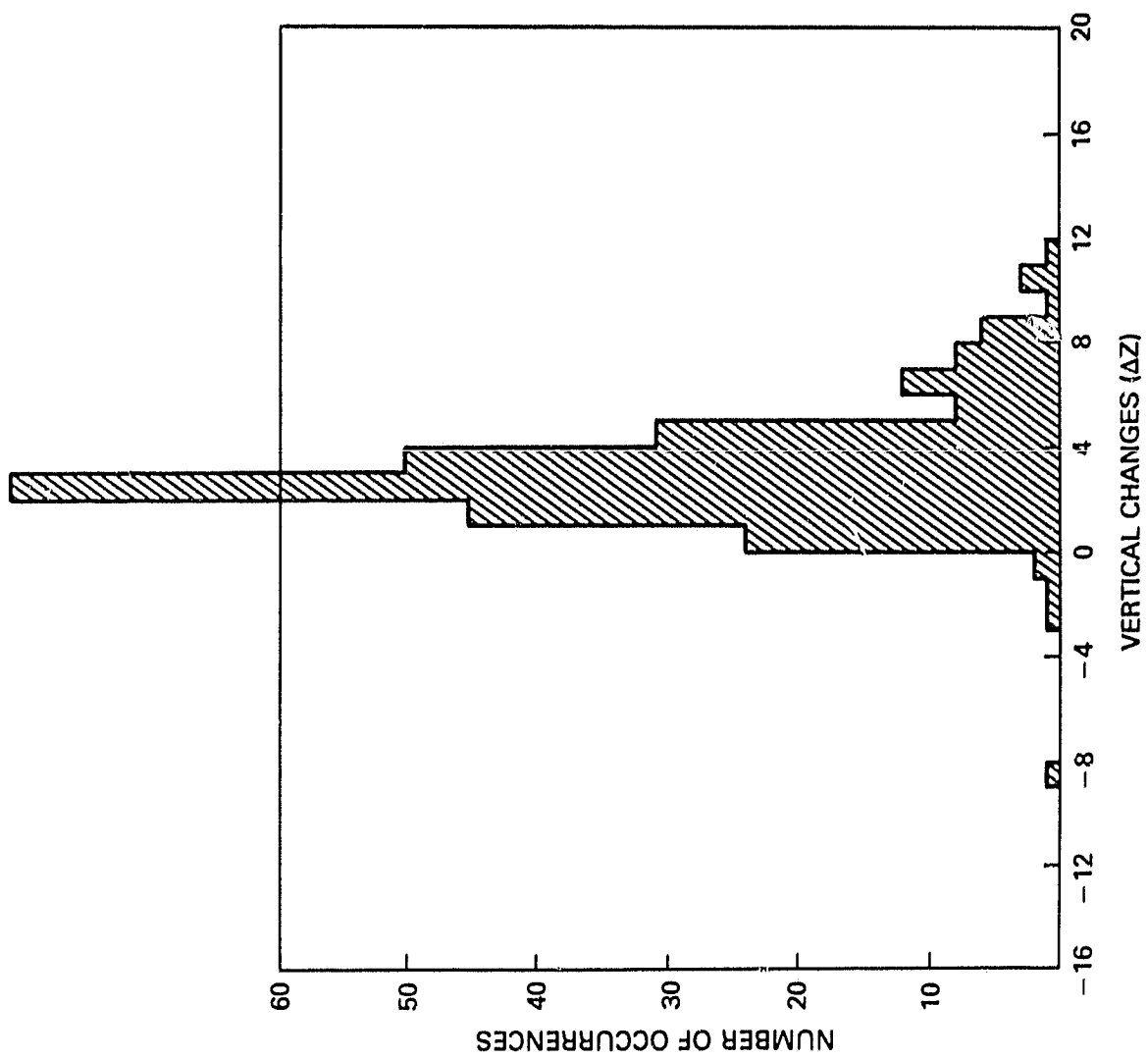


Figure C4. Changes in the vertical coordinate for channel B.

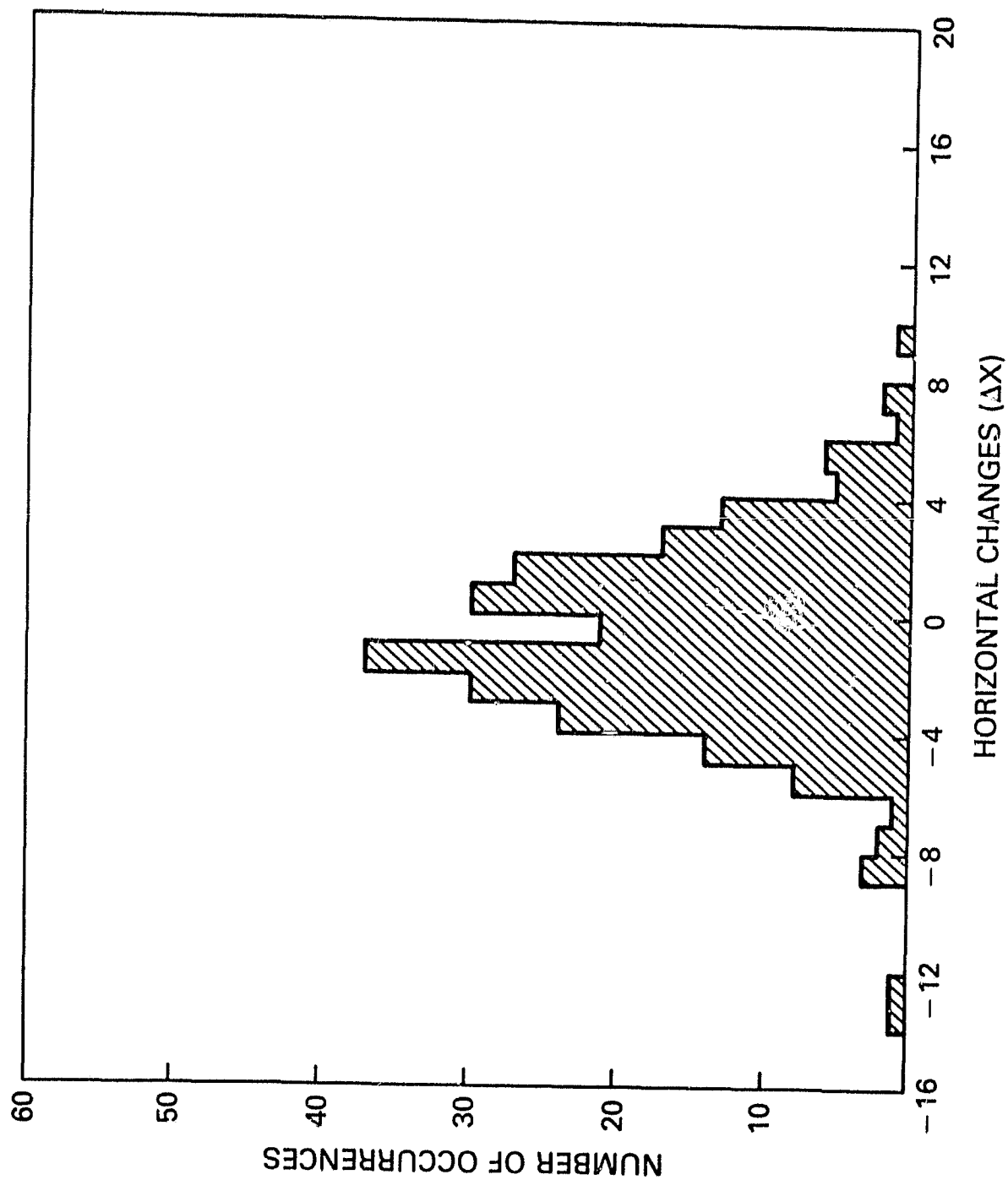


Figure C5. Changes in the horizontal coordinate for channel C.

ORIGINAL PAGE IS
OF POOR QUALITY

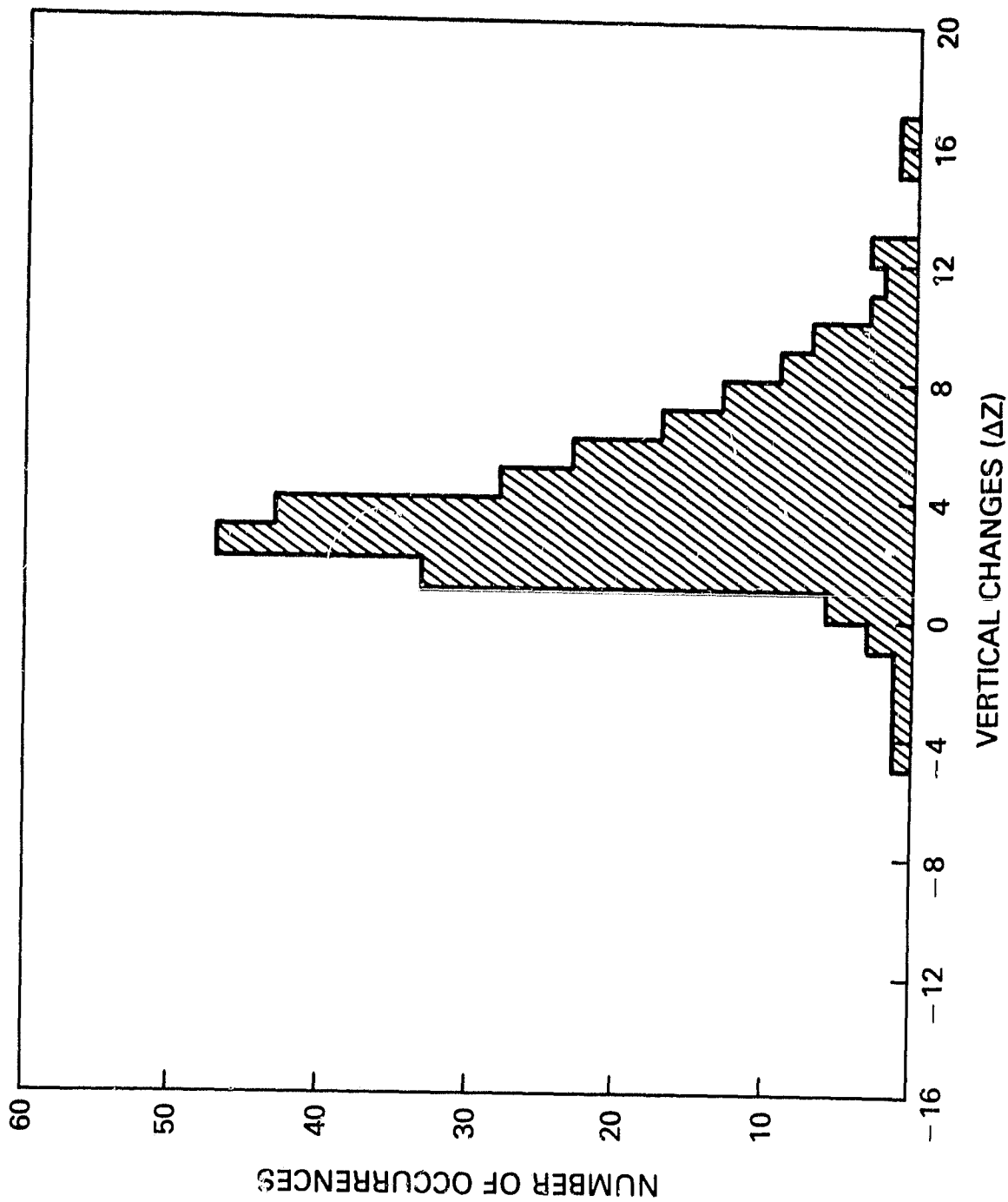


Figure C6. Changes in the vertical coordinate for channel C.

ORIGINAL PAGE IS
OF POOR QUALITY

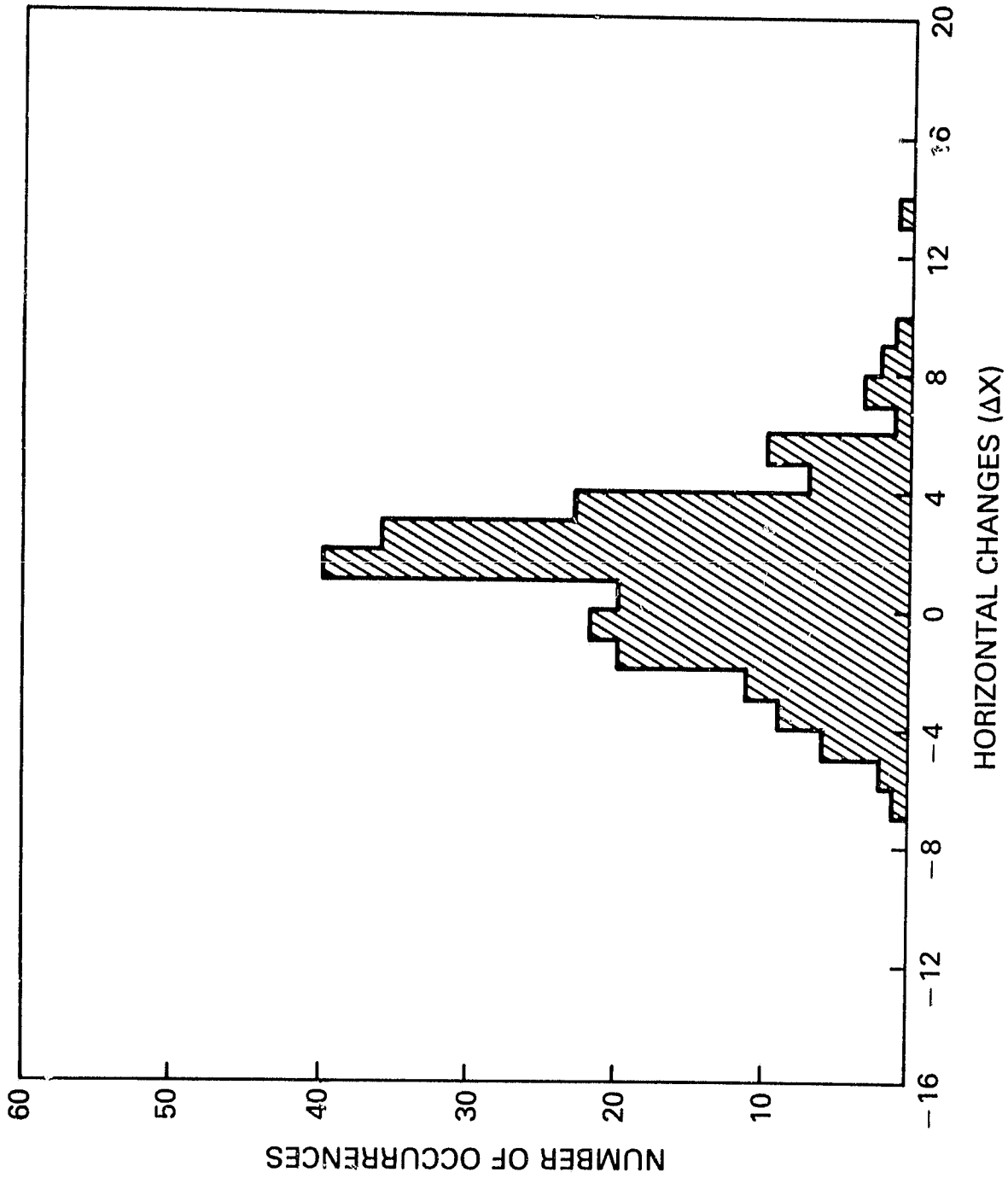


Figure C7. Changes in the horizontal coordinate for channel D.

ORIGINAL PAGE IS
OF POOR QUALITY

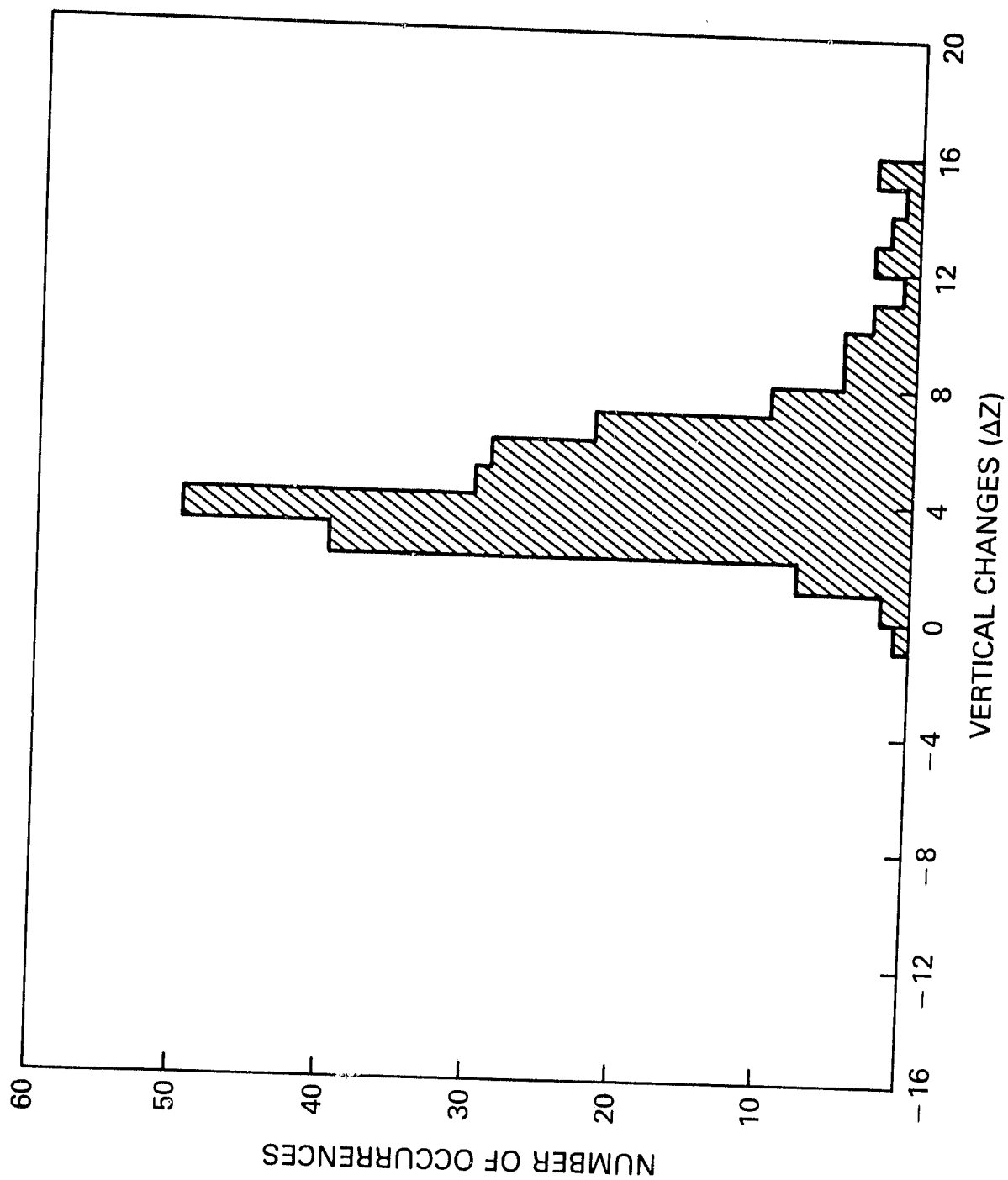


Figure C8. Changes in the vertical coordinate for channel D.

ORIGINAL PAGE 17
OF POOR QUALITY

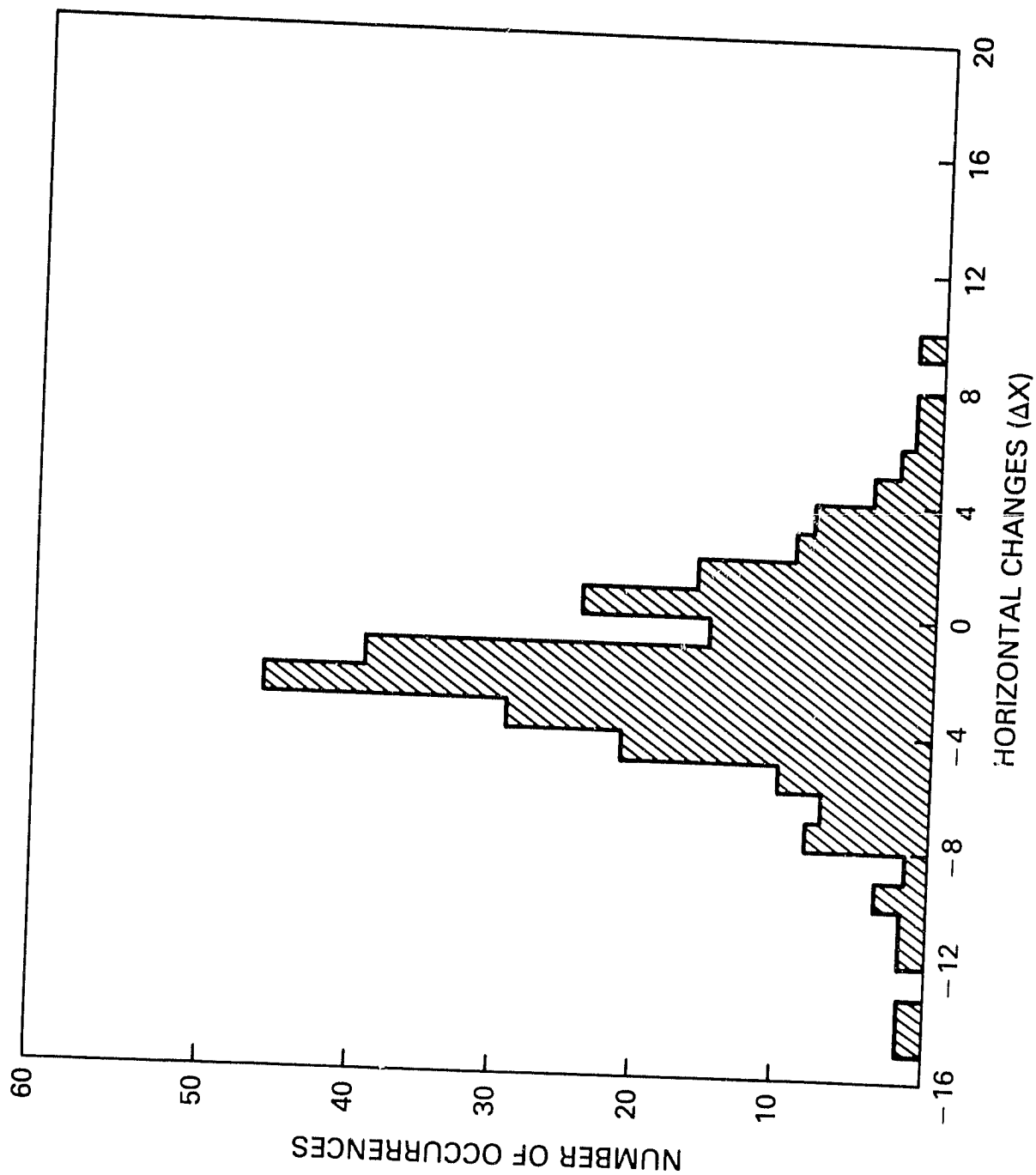


Figure C9. Changes in the horizontal coordinate for channel E.

ORIGINAL PAGE 13
OF POOR QUALITY

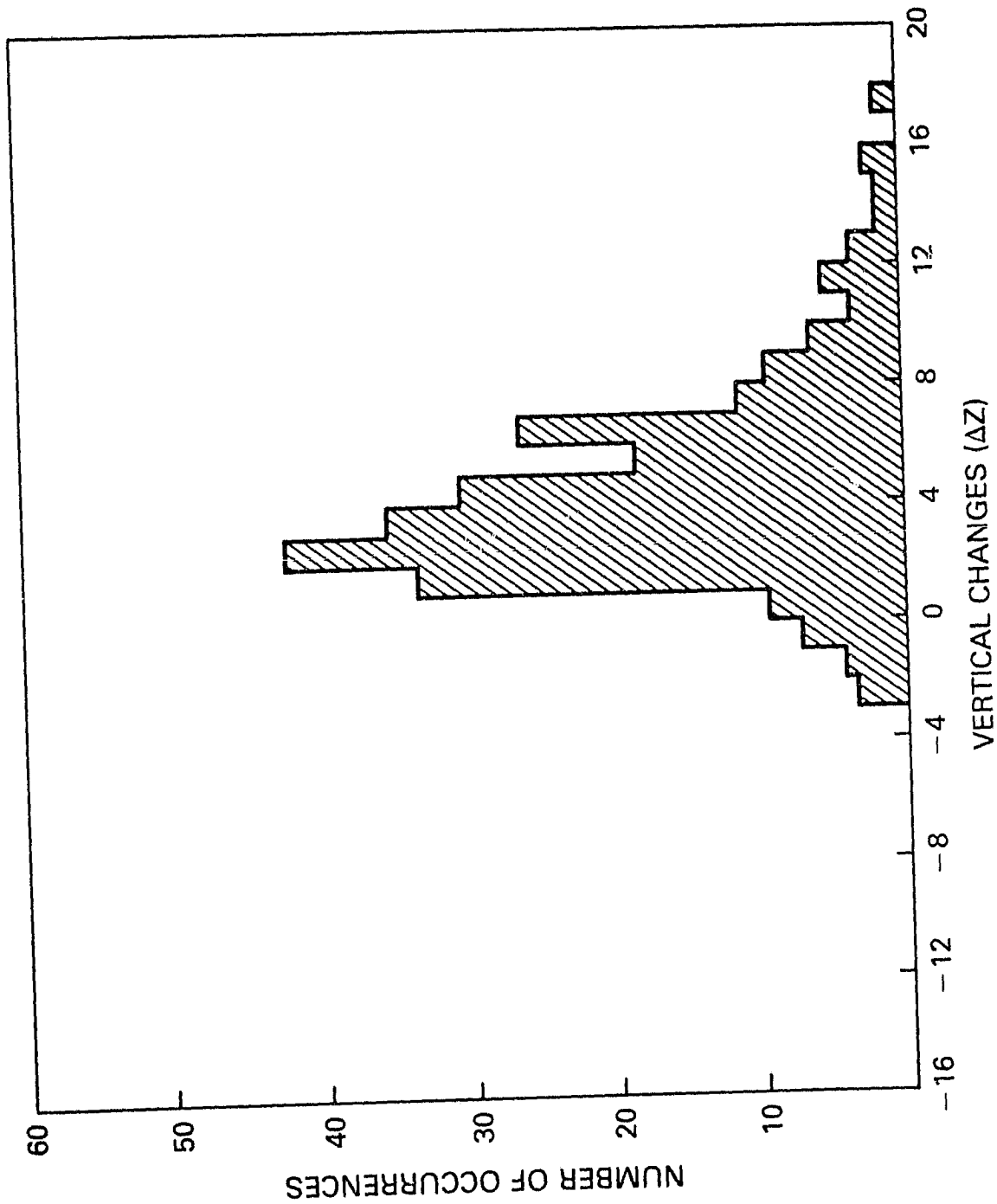


Figure C10. Changes in the vertical coordinate for channel E.

ORIGINAL PAGE IS
OF POOR QUALITY

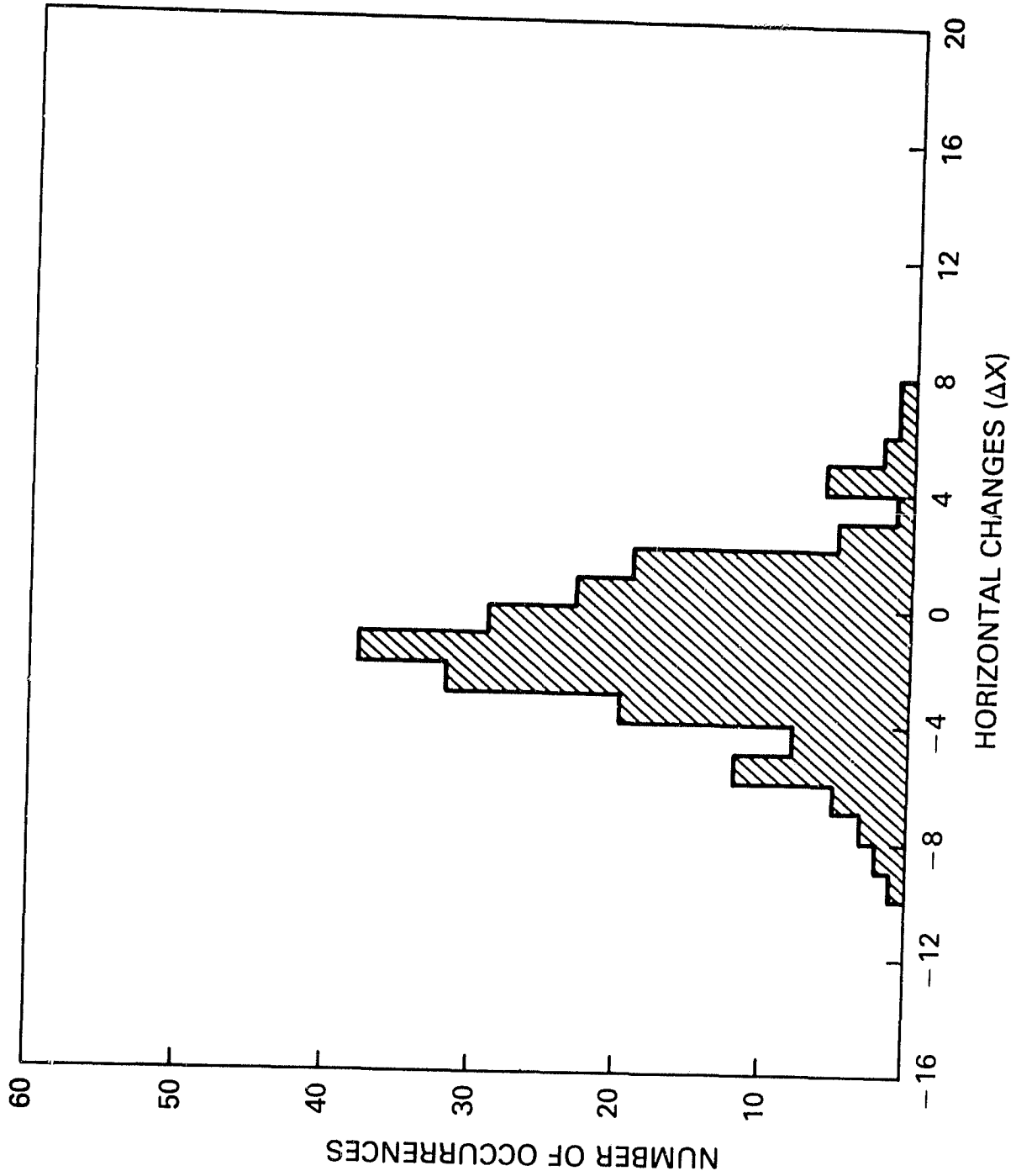


Figure C11. Changes in the horizontal coordinate for channel F.

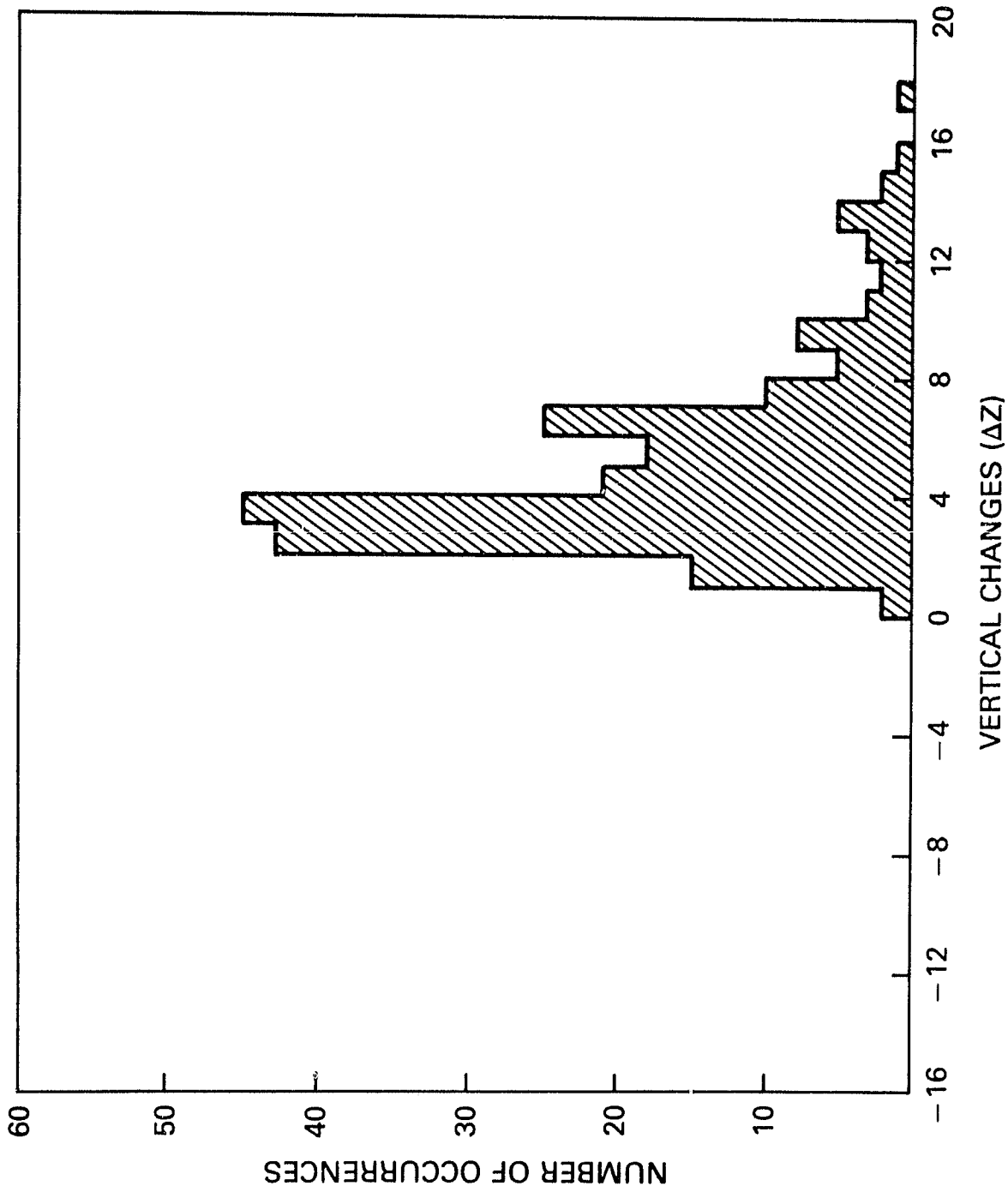


Figure C12. Changes in the vertical coordinate for channel F.

ORIGINAL PAGE IS
OF POOR QUALITY

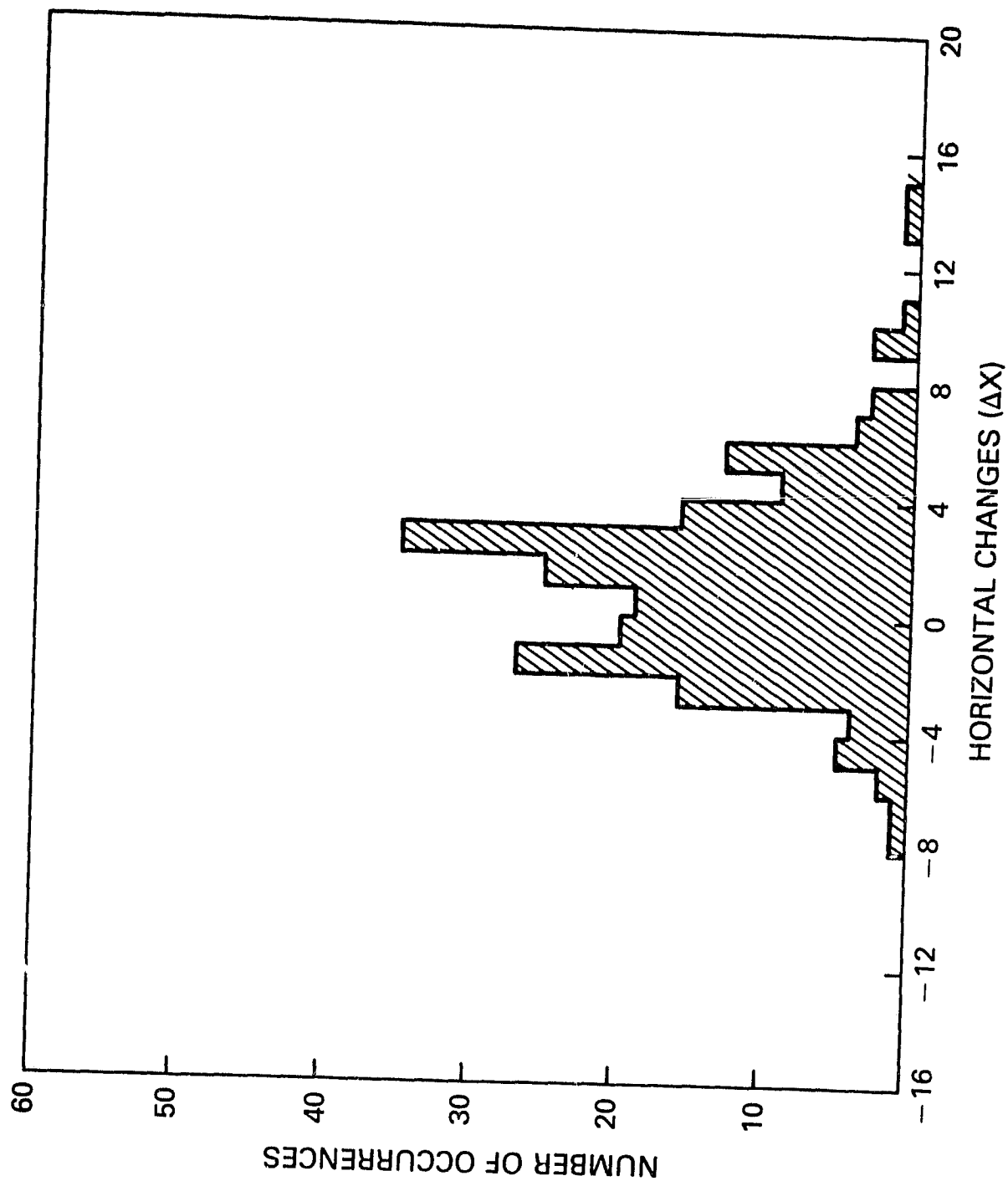


Figure C13. Changes in the horizontal coordinate for channel G.

ORIGINAL FILED
OF POCC BUREAU

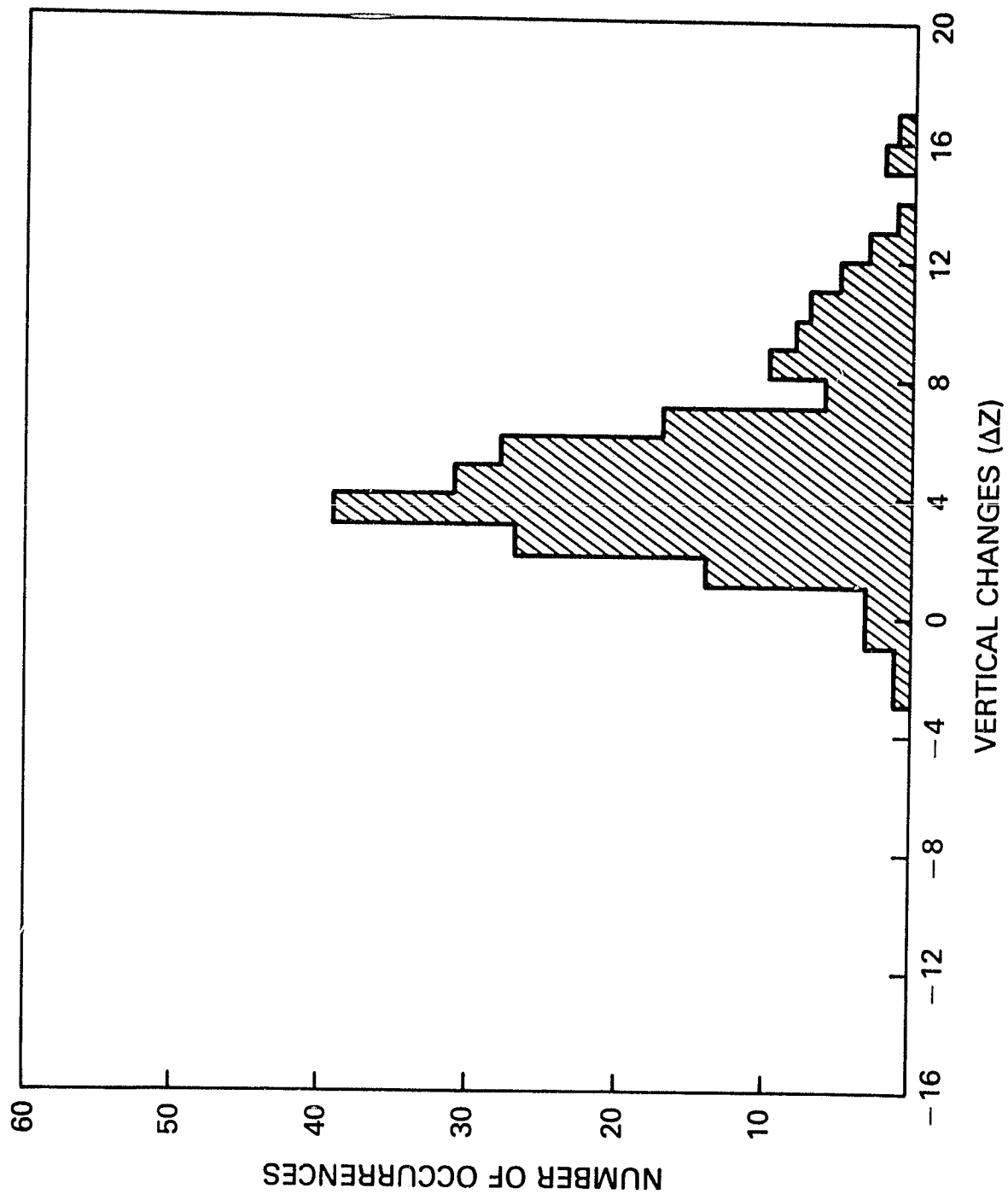


Figure C14. Changes in the vertical coordinate for channel G.

ORIGINAL PART 10
OF POOR QUALITY

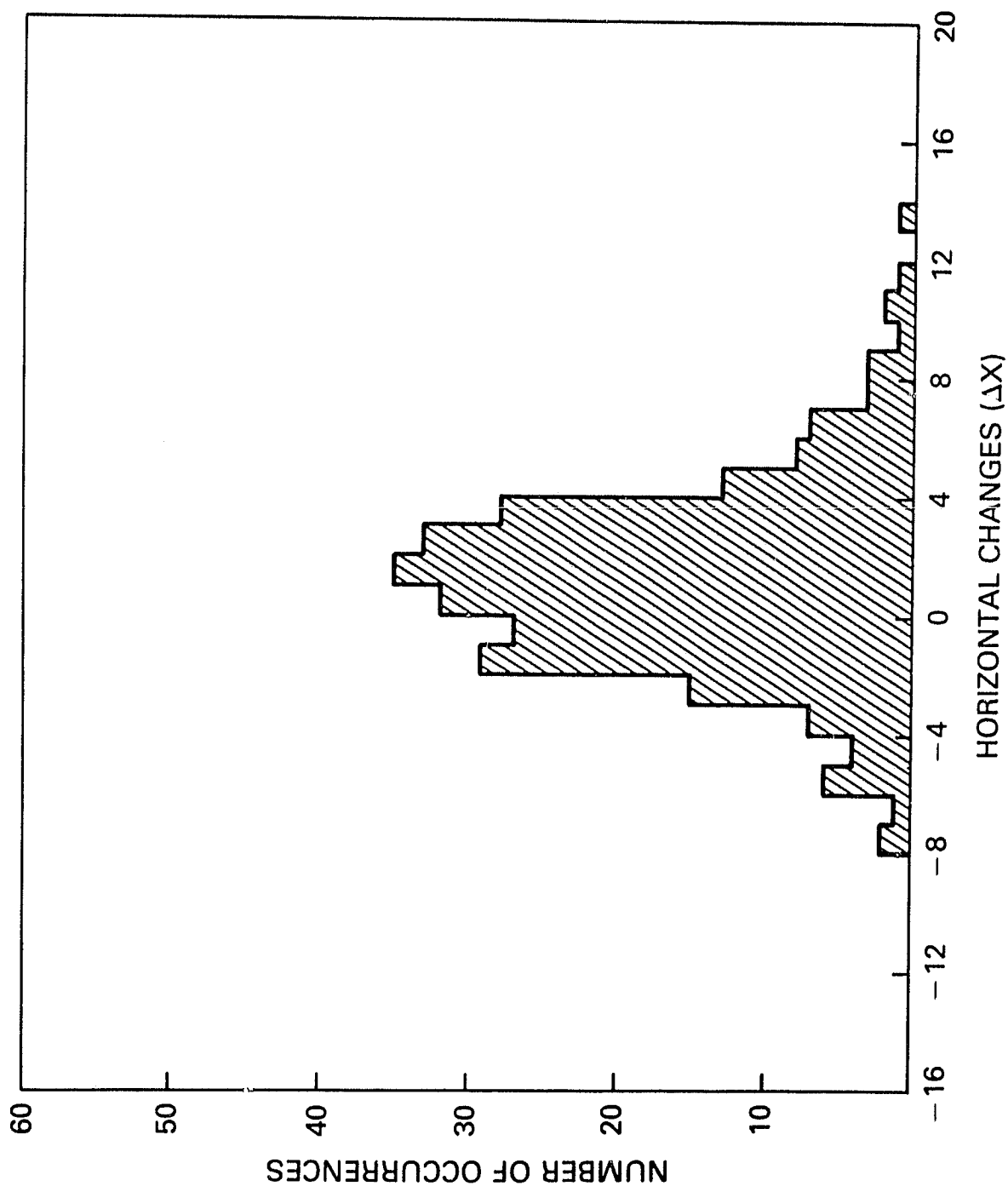


Figure C15. Changes in the horizontal coordinate for channel H.

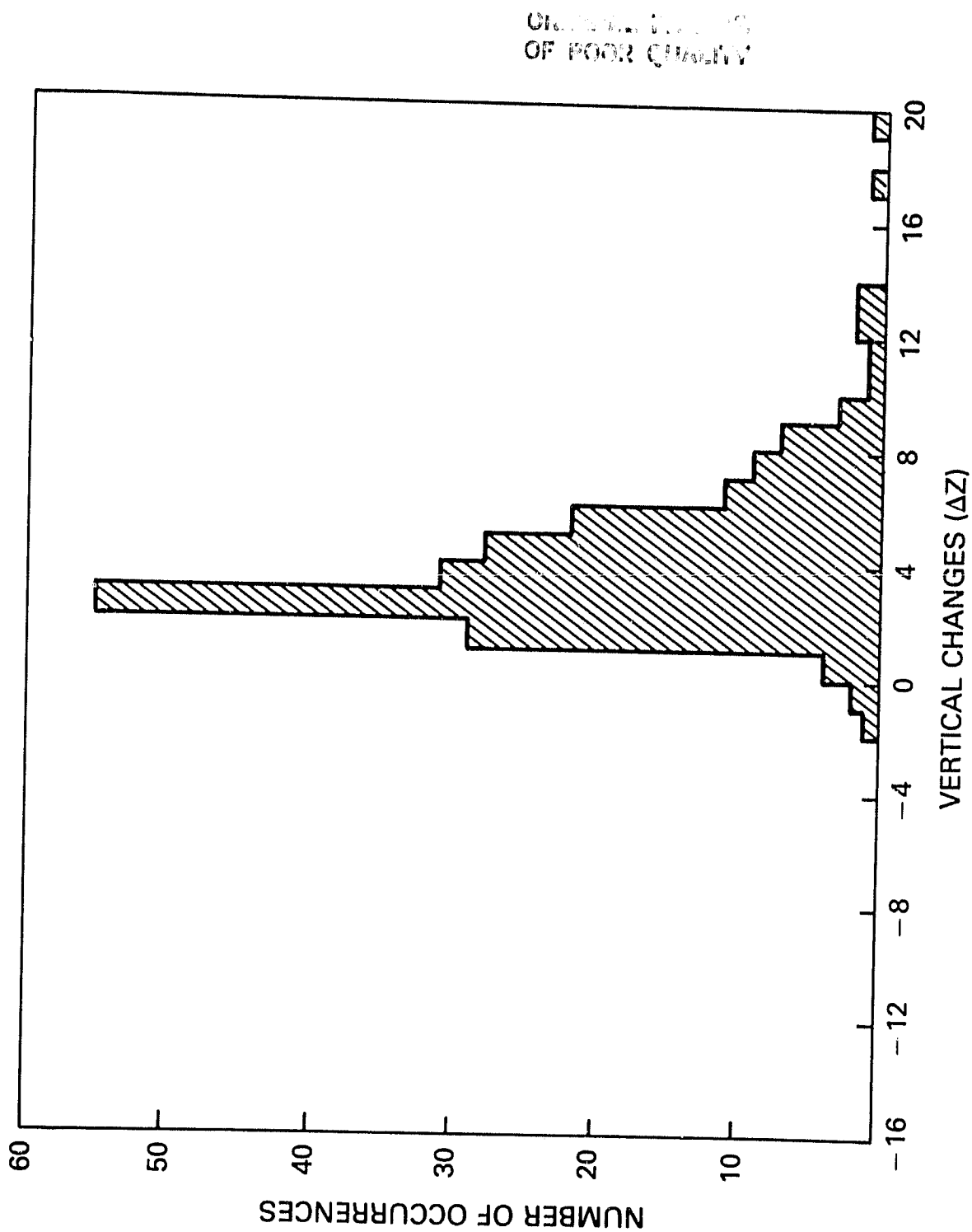


Figure C16. Changes in the vertical coordinate for channel H.